Joint Modeling of TDD and Decoupled Uplink/Downlink Access in 5G HetNets with Multiple Small Cells Deployment

Bachir Lahad, Marc Ibrahim, Samer Lahoud, Kinda Khawam, and Steven Martin

Abstract—Due to highly variant traffic in downlink (DL) and uplink (UL) in heterogeneous networks (HetNets), dynamic time-division duplexing (TDD) is proposed to dynamically allocate UL and DL resources. Under the same circumstances, downlink and uplink decoupled access (DUDA) is introduced to balance between UL and DL transmissions and to further improve the system performance. Rather than belonging to a specific cell, a mobile user can receive the downlink traffic from one base station (BS) and send uplink traffic through another BS. In this paper, we analytically investigate a joint TDD and DUDA statistical model with multiple small cells deployment. This model is based on a geometric probability approach. Taking all possible TDD subframes combinations between the macro and small cells, coupled and decoupled cell associations strategies are investigated in details. We derive analytical expressions for the capacity and the interference, considering a network of one macro cell and multiple small cells. We build on the derived capacity expressions to measure the decoupling gain and thus, identify the location of the interferer small cell where the decoupled mode maintains a higher gain in both DL and UL. Monte-Carlo simulations results are presented to validate the accuracy of the statistical model.

Index Terms—Wireless communications, cellular networks, downlink and uplink decoupled access, HetNets, TDD, 5G, spectral efficiency, cell association, capacity analysis.

1 Introduction

The rapid growth in wireless data traffic and bandwidth-intensive services (video streaming, live streaming, etc.) necessitates finding viable solutions to improve service quality and maximize the network performance. To accommodate these bandwidth intensive applications, an imperative shift from classical HetNets to next-generation HetNets (5G) is emerging in the aim of improving overall system performance. Because of the difference in uplink (UL) and downlink (DL) traffic loads expected in the next HetNets generation, it becomes essential to dynamically adjust UL/DL resources. To support this new approach, dynamic time-division duplexing (TDD) ([1], [2]) has been proposed. Several network performance metrics can be studied and statistically modeled to analyze a TDD based HetNet. Since the full reuse of spectrum has been advocated, an important metric and key performance factor in cellular networks is the Inter-Cell Interference (ICI). Statistical modeling of ICI plays a vital role in evaluating the system performance metrics and developing efficient interference mitigation techniques for cellular networks. In this work, the interference incurred at one tier (reference small cell) arising from the other tier (macro cell) is referred to as cross-tier interference. It may also be worth mentioning that, since multiple small cells are being deployed in real scenarios as an overlay to the macro cell, the modeling of the interference incurred at the reference small cell arising from other small cells is becoming essential to evaluate the overall system performance. In this paper, this type of interference is referred to as co-tier interference.

Nevertheless, the importance of UL arises along with the evolution of social networking and cloud solutions. Therefore, it is of great interest to introduce novel techniques that mitigate UL interferences, improve UL and DL throughputs and allow as well, a better use of radio resources by providing adequate load balancing among UL and DL. Such an additional feature is the decoupled UL/DL access ([3], [4]). According to many studies, the decoupling technique is expected to play an imperative role in the 5G architecture design. As stated in [5], the decoupling of the downlink and uplink is an emerging paradigm which will likely impact 5G design efforts. As mentioned in [6] and in order to achieve extremely high spectral efficiency in 5G, three enabling technologies which are massive MIMO, mmWave and densified HetNets with decoupling technique, are mainly concerned. Moreover, according to 3GPP Release 16 [7], TDD is widely used in 5G networks especially with high frequency bands. One of the main TDD features is the channel reciprocity, that helps in reducing the channel estimation overhead resulting from the MIMO technology and the multiple antennas implemented in 5G. Consequently, it is paramount to jointly model both TDD and decoupling technologies, as they are expected to play an important role in 5G HetNets.

Deriving closed-form expressions for cross-tier/co-tier interference and user capacity in TDD HetNets helps in designing and optimizing advanced enhancement techniques, including but not limited to the decoupled access technique. Deriving these expressions reduces as well the need for time consuming Monte-Carlo simulations, especially in the case of multiple small cells deployment where the time

- *B. Lahad, M. Ibrahim and S. Lahoud are with Saint Joseph University of Beirut, Faculty of Engineering, ESIB, Mar Roukos, Lebanon.*
- *K. Khawam is with University of Versailles, Versailles, France.*
- *S. Martin is with University of Paris Sud, LRI Laboratory, Orsay, France.*

required to run Monte-Carlo simulations significantly increases. Hence, the focus of this paper is to develop a joint TDD/decoupling model and to highlight the benefits that the decoupling access mode can bring to a HetNet TDD based system, in terms of UL and DL spectral efficiencies. More insight into the benefits of decoupling mode in multiple small cells environment, is provided in this work in terms of UL and DL decoupling gains.

1.1 Related Work

The problem of interference and capacity modeling in HetNets has been tackled recently using several approaches, in which closed-form formulas are derived to compute main network performance metrics. Some of these studies tackled solely the downlink case, other works considered only the uplink case.

For the downlink case, a semi-analytical distribution for the signal-to-interference-noise ratio (SINR) has been derived in [8] under path loss and log normal shadowing for femtocell networks. In [9], the applicability of the Gaussian and binomial distributions for modeling the downlink ICI is investigated. In [10], an analytical approach based on geometric probability was developed for downlink performance analysis of a HetNet network model where the coverage probability and the spectral efficiency have been derived and verified by simulation. A novel circular interference model was introduced in [11] to facilitate statistical analysis in networks with regular grid layout. The key idea was to spread the power of interferers uniformly along the circumcircle of the grid-shaping polygon.

Several research works for the uplink appear in [12], [13] and [14]. In [15], a new approach based on Gaussian approximation was introduced to analyze the uplink signal to interference ratio (SIR) performance. In [16], the scheduling-based interference models for LTE networks was considered where the distance distribution and thus the interference distribution was derived for different resource allocation schemes such as proportional fair, greedy and round robin scheduling schemes. In [17], uplink capacity (in bps/Hz) was derived with closed-form expressions in both dedicated and shared spectrum access scenarios. The proposed framework exploited the distance distributions based on geometric probability theory to characterize the co-tier and cross-tier uplink interferences.

As for the modeling of interference in TDD systems, the work in [18] introduced a statistical framework to analyze uplink/downlink interactions where analytical expressions for the four interference types in TDD systems were derived. For interference-aware scenarios, the distribution of the distance between the source and victim of interference was based on the scheduling algorithms defined in [16]. Note that the work in [18] did not evaluate important network performance metrics such as average cell capacity. Instead, interference maps were generated to analyze the impact of TDD operation in a given network. In [19], an analytical framework was developed to evaluate the performance of a TDD system in HetNets in terms of UL and DL spectral efficiencies, and to model the concurrent uplink and downlink transmission signals in two different types of cells, macro and small cells. This model considered a network consisting of one macro cell and one small and did not investigate the case of multiple small cells environment.

In a different research thread, there are a lot of works that have introduced the concept of downlink/uplink decoupling in cellular systems. The work in [20] focused on the architectural design and realization, identified and explained some key arguments in favor of DUDA.

A group of articles studied various link association policies and showed their performances based on simulations results. In [21], the notion of DUDA is studied, where the downlink cell association is based on the downlink received power, while the uplink is based on path loss. The follow-up work in [22] considered the cell-load as well as the available back-haul capacity within the association process. The work in [23] added a cell selection offset to the reference signals in small cells.

Other works focused on the analytical evaluation of a predefined association policy. The research work in [24] and [25] focused on the analytical characterization of the decoupled access, relying on the stochastic geometry framework and applying a specific association criteria (power received or transmitted). Uplink performance improvement brought by a DUDA mode over a conventional coupled UL/DL access mode (CUDA), was investigated in [26]. A general analytical framework in a hybrid system (sub-6GHz and millimeter wave) was developed in [27] where the biased uplink and downlink cell association, as well as the rate coverage probability, are derived.

1.2 Contributions and Organization

In this paper, we develop a general model for interference and user capacity in TDD HetNets for various link association policies. This model is based on a geometric probability approach and considered the modeling of both cross-tier and co-tier interferences in a multiple small cells environment.

The main contributions of this work can be summarized as follows:

1) TDD Statistical Model in Multiple Small Cells HetNets: We consider analyzing, in this paper, both uplink/downlink interactions, whereas other works introduced either a downlink ICI model as in [9] and [10] or an uplink ICI model as in [16] and [17]. Few studies considered modeling a TDD system, however they either did not consider a HetNet system and did not evaluate any network performance indicator as in [18] or they were limited to one small cell case study as in [19]. In this paper, operating a TDD-based HetNet network necessitates four interference scenarios depending mainly on the geographical distance between the reference cell and the neighboring cell. In a multiple small cells scenario, the neighboring cell can be either the small cell or the macro cell. Thus, analyzing four interference scenarios is still applicable because of the TDD subframes distribution that is considered perfectly synchronized between the small cells.

2) Analytical Model Covering Various User Association Policies: Focusing on the decoupled access strategy, other similar works either developed an analytical

This article has been accepted for publication in a future issue of this journal, but has not been fully edited. Content may change prior to final publication. Citation information: DOI 10.1109/TMC.2020.2979447, IEEE Transactions on Mobile Computing

model studying one specific association criteria ([24]- [27]) or investigated multiple association strategies based on simulation results ([21]- [23]). In this work, an analytical model covering four association policies is developed with the aim of studying the improvement that the decoupling access can bring to TDD HetNets among all other association policies.

3) Joint Modeling of TDD and Decoupled UL/DL access in Multiple Small Cells HetNets: Studying the next-generation wireless 5G HetNets with respect to TDD and UL/DL decoupled access. Other works investigated either a TDD system as in [18] and [19] or the decoupled access technique as in [21]- [27]. In fact, considering a TDD scenario jointly with a decoupled association policy appears to be a viable solution to address UL and DL throughput degradation challenges.

The rest of the paper is organized as follows. In Section 2, we introduce some basic notations and the system model of coupled and decoupled modes in TDD HetNet with multiple small cells deployment. In Section 3, we develop a statistical framework to model the cross-tier and co-tier interferences in multiple small cells TDD HetNets, closed-form expressions are derived to measure the average cell capacity. Four association strategies are modeled in Section 4 to assess the improvement brought by DUDA mode to TDD HetNets, in terms of UL and DL spectral efficiencies. In Section 5, closed-form expressions to characterize the interference are derived and user capacity is analyzed to examine the impact of applying the decoupled access policy in a multiple small cells TDD HetNet. The overall system performance is evaluated by measuring the uplink/downlink decoupling gains. In Section 6, we present analytical results as well as simulation results to evaluate the system performance in various realistic scenarios. Finally, the conclusion of the paper is given in Section 7.

2 System Model

We consider a two-tier heterogeneous cellular network consisting of one macro cell and multiple small cells. We denote by N_s the number of small cells. In the coming sections, the radius of the macro cell and the small cell will be denoted by R and R_s respectively. Let R_e be the radius of the expanded area, a tunable variable in Section 4. We denote by d_{12} the distance from the reference small cell to the interfering small cell to be a new design parameter in Section 5.

A new area, considered as an extension to the small cell average zone, will be studied in the aim of analyzing the impact of the decoupled UL/DL access and other access policies on the users located inside and outside this expanded area. Users inside this area are located at a distance r from the center of the reference small cell where $R_s < r < R_e$. In order to investigate the impact of each association policy, users inside the expanded area can be either coupled or decoupled at a specific time t.

For each association policy and in order to characterize the concurrent cross-tier and co-tier interferences in a TDD HetNet, the proposed model mandates analyzing four interference scenarios by considering all UL/DL TDD possible combinations between the macro cell from a side and the small cells from the other side. Small cells are considered synchronized with the same TDD configuration. For example, Up - Down scenario defines a situation where the macro cell is operating in the uplink and the small cells in the downlink. Same logic applies to define the other three scenarios.

Macro users are uniformly distributed in the macro cell. Similarly, small cell users are uniformly distributed inside their respective small cell. The reference small cell is located at a distance d from the center of the macro cell. The interfering small cell is located at a distance d_{12} and d_2 from the reference small cell and the macro cell respectively. Figure 1 displays all possible desired links and interfering links for which statistical expressions are derived in the next sections. In the following, we will define the major notations of these links:

- $\psi = \{s, m, i\}$ denotes a set of base stations. The small cell reference BS is designated by s, the interfering macro cell BS by m and the interfering small cell BS by i. Note that e designates the expanded area at the reference small cell s.
- The interference experienced from the macro cell m and the interfering small cell i at the reference small cell s, is denoted by I_m and I_i respectively.
- The transmission power of the macro BS and the small cell BS is denoted by P_m and P_s respectively.
- The transmission power of the macro user and the small cell user is denoted by P_{um} and P_{us} respectively.
- $u_{k,j}$ denotes the distance from the user in the cell k to the user in the cell j, where j and $k \in \psi$.
- $r_{k,j}$ denotes the distance from the cell k to the user in the cell j, where j and $k \in \psi$. If k=j, $r_{k,j} = r_k$.
- $d_{k,j}$ denotes the distance from the cell k to the cell j, where j and $k \in \psi$.

For simplicity, we redefine $d_{k,j}$ notations in Table 1.

TABLE 1
$d_{k,j}$ Notations

$d_{k,j}$ = d; k=m & j=s	Distance between the macro cell and the reference small cell
$d_{k,j} = d_{12}$; k=s & j=i	Distance between the reference small cell and the interfering small cell
$d_{k,j} = d_2$; k=m & j=i	Distance between the macro cell and the interfering small cell

Remark 1 (Composite Fading): In this work, the composite fading denoted by K is considered as a constant. It combines both the shadowing and the fading.

Nonetheless, we have simulated exactly the same scenarios under a variable fading. Accordingly, a log-normal shadowing and an exponential distribution with parameter $\lambda = 1$ as an approximation of the Rayleigh fading, were considered. As a result, we obtained nearly the same throughput values in UL and DL and same observations as in the case of a constant composite fading; the impact of the decoupling in comparison with other association policies remained the same. Consequently, a constant fading was adopted in this study.

This article has been accepted for publication in a future issue of this journal, but has not been fully edited. Content may change prior to final publication. Citation information: DOI 10.1109/TMC.2020.2979447, IEEE Transactions on Mobile Computing

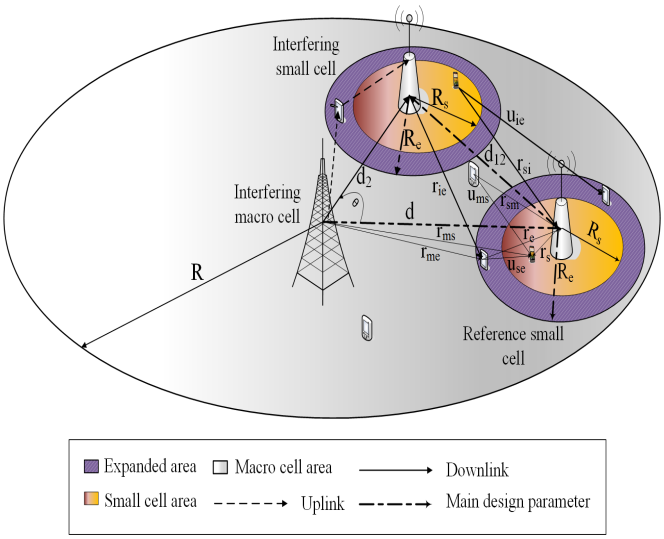

Fig. 1. Geometrical illustration of all possible links distribution.

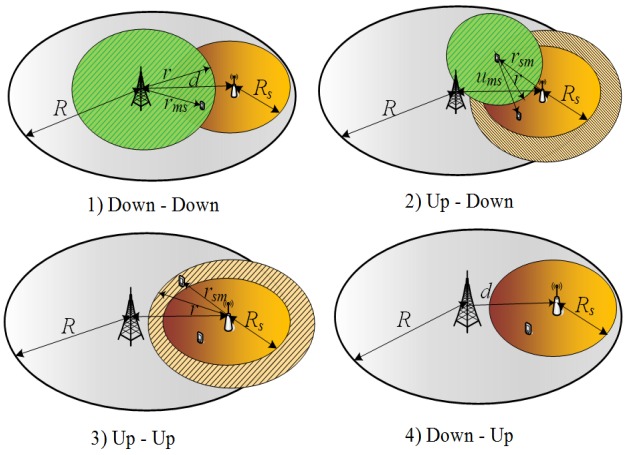

Fig. 2. Geometrical illustration of the four interference types.

3 TDD Statistical Model in Multiple Small Cells HetNets

In order to characterize the statistics of each interference scenario that could occur in TDD-based HetNets, the proposed framework mandates analyzing in details both the cross-tier and co-tier interferences in multiple small cells environment.

3.1 Cross-tier Interference Modeling

Cross-tier interference is the interference experienced from the macro cell m at the reference small cell s. In this section, analytical expressions for the four interference types are derived based on a geometric approach adopting the *cells intersections* method (see Fig. 2 for illustration). In order to apply this method, the following two assumptions in regards to the topology and users distribution must be considered:

- Macro cell is an area with radius R that englobes small cells with radius Rs each.
- Users are uniformly distributed inside each of the aforementioned cells.

3.1.1 Down - Down (BS-MS interference)

The downlink interference from the macro BS to the mobile user associated with a small BS is defined as follows:

$$I_m = KP_m r_{ms}^{-\gamma},$$

where γ is the path-loss exponent and K the composite fading channel. The probability density function (PDF) of r_{ms} and thus, the PDF of I_m are derived based on the closed-form expressions obtained in [19]:

$$f_{r_{ms}}(r) = \frac{1}{\pi R_s^2}(\pi r - 2r\arcsin(\frac{d^2+r^2-R_s^2}{2dr})), \quad (1)$$

$$f_{I_m}(x) = \frac{1}{x\gamma} f_{r_{ms}}\left((\frac{x}{C})^{-\frac{1}{\gamma}}\right)(\frac{x}{C})^{\frac{-1}{\gamma}}, \quad (2)$$

where $C = KP_m$.

3.1.2 Up - Down (MS-MS interference)

The downlink interference from the macro user to the small cell user is defined as follows:

$$I_m = KP_{um} u_{ms}^{-\gamma}.$$

The PDF of u_{ms} is derived by replacing r_0 with u_{ms} in the closed-form expression obtained for $f_{r_0}(r)$ in [19]:

$$f_{u_{ms}}(r) = \int_{r-R_s}^{r+R_s} f_{u_{ms}}(r)_{|r_{sm}} f_{r_{sm}}(r_{sm}) dr_{sm}, \quad (3)$$

where $f_{u_{ms}}(r)_{|r_{sm}} = \frac{1}{\pi R_s^2}(\pi r - 2r\arcsin(\frac{r_{sm}^2+r^2-R_s^2}{2r_{sm}r}))$ and $f_{r_{sm}}(r_{sm})$ defined as follows:

$$f_{r_{sm}}(r_{sm}) = \begin{cases} \frac{1}{\pi R^2 - \pi R_s^2}(2\pi r_{sm}), & R_s \le r_{sm} < R-d \\ v(r_{sm}), & R-d \le r_{sm} \le R+d, \end{cases} \quad (4)$$

where $v(r_{sm}) = \frac{1}{\pi R^2 - \pi R_s^2}(\pi r_{sm} - 2r_{sm}\arcsin(\frac{d^2+r_{sm}^2-R^2}{2dr_{sm}}))$.

Consequently, the PDF of I_m can be written as:

$$f_{I_m}(x) = \frac{1}{x\gamma} f_{u_{ms}}\left((\frac{x}{C})^{-\frac{1}{\gamma}}\right)(\frac{x}{C})^{\frac{-1}{\gamma}}, \quad (5)$$

where $C = KP_{um}$.

3.1.3 Up - Up (MS-BS interference)

The uplink interference from the macro user to the small cell BS is defined as follows:

$$I_m = KP_{um} r_{sm}^{-\gamma}.$$

The PDF of r_{sm} is given based on the closed-form expression derived in [19]:

$$f_{r_{sm}}(r) = \begin{cases} \frac{1}{\pi R^2 - \pi R_s^2}(2\pi r), & R_s \le r < R-d \\ s(r), & R-d \le r \le R+d, \end{cases} \quad (6)$$

where $s(r) = \frac{1}{\pi R^2 - \pi R_s^2}(\pi r - 2r\arcsin(\frac{d^2+r^2-R^2}{2dr}))$.

Consequently, the PDF of I_m can be written as:

$$f_{I_m}(x) = \frac{1}{x\gamma} f_{r_{sm}}\left((\frac{x}{C})^{-\frac{1}{\gamma}}\right)(\frac{x}{C})^{\frac{-1}{\gamma}}, \quad (7)$$

where $C = KP_{um}$.

3.1.4 Down - Up (BS-BS interference)

The uplink interference from the macro BS to the small cell BS is defined as follows:

$$I_m = KP_m d^{-\gamma}.$$

In this case, I is a constant. Accordingly, the moment generating function (MGF) of I_m will be defined as:

$$M_{I_m}(t) = \mathbb{E}[e^{(-tI_m)}] = e^{-tI_m}. \quad (8)$$

3.2 Co-tier Interference Modeling in Multiple Small Cells HetNets

In order to model the cumulative interference at the reference small cell in a multiple small cells HetNet, we derive hereafter closed-form expressions for the co-tier interference to complement the cross-tier interference expressions derived in the previous section. We consider as co-tier interference the interference experienced at the reference small cell s from the interfering small cell i (see Fig. 1). Since the small cells are considered synchronized in uplink and downlink, the following two scenarios must be taken into account to derive expressions for the co-tier interference:

3.2.1 Small cell in downlink mode

The downlink co-tier interference from the interfering small cell BS to the mobile user associated with the reference small BS is defined as follows:

$$I_i = KP_s r_{is}^{-\gamma}.$$

Similar to the BS-MS scenario in (1), the PDF of r_{is} can be written as:

$$f_{r_{is}}(r) = \frac{1}{\pi R_s^2}\Big(\pi r - 2r\arcsin(\frac{d_{12}^2 + r^2 - R_s^2}{2d_{12}r})\Big), \quad (9)$$

where $d_{12} - R_s \leq r \leq d_{12} + R_s$ and d_{12} represents in this case the distance between the centers of two intersecting circles.

3.2.2 Small cell in uplink mode

The uplink co-tier interference from the interfering small cell user to the reference small cell BS is defined as follows:

$$I_i = KP_s r_{si}^{-\gamma}.$$

The PDF of r_{si} can be obtained as a result of the cell intersection of radius r with the interfering small cell of radius R_s:

$$f_{r_{si}}(r) = \frac{1}{\pi R_s^2}\Big(\pi r - 2r\arcsin(\frac{d_{12}^2 + r^2 - R_s^2}{2d_{12}r})\Big), \quad (10)$$

where $d_{12} - R_s \leq r \leq d_{12} + R_s$.

Introducing additional small cells leads to a considerable change in the cross-tier interference expressions ((6) and (4)) derived within the Up - Up and Up - Down scenarios, i.e. scenarios where the main interferer is the macro user. In this context, the area occupied by these small cells should be excluded when deriving the cumulative distribution function (CDF) of the interference experienced from the macro user at the reference small cell. Based on [28], let $f(r)$ be the result of the intersection with the macro cell of radius R:

$$f(r) = \pi r - 2r\arcsin(\frac{d^2 + r^2 - R^2}{2dr}),$$

and $g(r)$ the result of the intersection with the interfering small cell of radius R_s:

$$g(r) = \pi r - 2r\arcsin(\frac{d_{12}^2 + r^2 - R_s^2}{2d_{12}r}).$$

Consequently, the PDF of r_{sm} in (4) and (6) is updated to include the distance between small cells (d_{12}) as follows:

$$f_{r_{sm}}(r) = \begin{cases} \frac{2\pi r}{\pi R^2 - 2\pi R_s^2}, & R_s \leq r < R - d \\ \frac{f(r)}{(\pi R^2 - 2\pi R_s^2)}, & R - d \leq r \leq d_{12} - R_s \\ \frac{f(r) - g(r)}{(\pi R^2 - 2\pi R_s^2)}, & d_{12} - R_s \leq r \leq d_{12} + R_s \\ \frac{f(r)}{(\pi R^2 - 2\pi R_s^2)}, & d_{12} + R_s \leq r \leq R + d. \end{cases} \quad (11)$$

Model Scalability: Although in this work the model is built with two small cells, however its scope can be expanded to include multiple small cells interferers i located at distance d_{1i} from the macro cell respectively. Accordingly, in order to derive expressions for the interference experienced from different small cells interferers, the PDF of r_{is} in (9) is revised by replacing d_{12} with d_{1i}, same for the PDF of r_{si} in (16). On the other hand, the PDF of the interference experienced from the macro users and thus, the PDF of r_{sm} in (11) is carefully revised and can be written as follows:

$$f_{r_{sm}}(r) = \begin{cases} \frac{2\pi r}{\pi R^2 - N_s \pi R_s^2}, & R_s \leq r < R - d \\ \frac{f(r)}{(\pi R^2 - N_s \pi R_s^2)}, & R - d \leq r \leq d_i - R_s \\ \frac{f(r) - \sum_{i=2}^{N_s} g_i(r)}{(\pi R^2 - N_s \pi R_s^2)}, & d_i - R_s \leq r \leq D_i + R_s \\ \frac{f(r)}{(\pi R^2 - N_s \pi R_s^2)}, & D_i + R_s \leq r \leq R + d, \end{cases} \quad (12)$$

where $f(r) = \pi r - 2r\arcsin(\frac{d^2 + r^2 - R^2}{2dr})$, $D_i = \max\limits_{2 \leq i \leq N_s} d_{1i}$, $d_i = \min\limits_{2 \leq i \leq N_s} d_{1i}$ and

$$g_i(r) = \begin{cases} \pi r - 2r\arcsin(\frac{d_{1i}^2 + r^2 - R_s^2}{2d_{1i}r}), & d_{1i} - R_s \leq r \leq d_{1i} + R_s \\ 0, & elsewhere. \end{cases}$$

3.3 PDF and MGF of the Signal of Interest

The signal power received by a randomly selected user at the reference small cell on a downlink channel is defined as: $S = KP_s r_s^{-\gamma}$ where r_s is the distance of the user from the small BS s. The PDF of the received signal S is given based on the closed-form expression derived in [19]:

$$f_S(x) = \beta x^{-(\frac{2+\gamma}{\gamma})}, \quad (13)$$

where $\beta = \frac{2C^{\frac{2}{\gamma}}}{\gamma R_s^2}$ and $C = KP_s$. Note that same logic applies to derive similar expressions on the uplink channel.

3.4 Analytical Evaluation of Ergodic Capacity

The average user capacity per unit bandwidth i.e. the spectral efficiency at the reference small cell, in a multiple small cells environment is defined as the achievable average rate of the link to the allocated bandwidth (B), expressed mathematically by the modified Shannon's formula as:

$$C = \mathbb{E}\Big[\frac{B\ln(1 + \frac{S}{I_{tot} + \sigma^2})}{B}\Big] = \mathbb{E}\Big[\ln(1 + \frac{S}{I_{tot} + \sigma^2})\Big], \quad (14)$$

where σ^2 is the thermal noise power variance and I_{tot} the cumulative interference defined as: $I_{tot} = I_m + I_i$. S and

This article has been accepted for publication in a future issue of this journal, but has not been fully edited. Content may change prior to final publication. Citation information: DOI 10.1109/TMC.2020.2979447, IEEE Transactions on Mobile Computing

I_{tot} are considered as two independent variables. In the following, we will provide a proposition to approximate the generic function of the capacity C:

Proposition 1: The capacity C can be approximated by expressing it in terms of the weights w_e and abscissas x_e of a Laguerre orthogonal polynomial as follows:

$$C = \sum_{e=1}^{n} w_e \Big(\frac{M_{I_m}(x_e/(\sigma^2+a)) M_{I_i}(x_e/(\sigma^2+a))}{x_e e^{-(a x_e)/(\sigma^2+a)}} - \frac{M_S(x_e/(\sigma^2+a)) M_{I_m}(x_e/(\sigma^2+a)) M_{I_i}(x_e/(\sigma^2+a))}{x_e e^{-(a x_e)/(\sigma^2+a)}} \Big), \tag{15}$$

where a is a parameter introduced to solve the convergence issue faced when deriving the MGF expressions of I_m and I_i.

Proof of Proposition 1: The interference, in general, can be written as: $I = KPr^{-\gamma} = Cr^{-\gamma}$ where $C = KP$, r denotes the interfering link distance, P the transmitted power and K the composite fading. Applying the chain rule to the CDF of I, the corresponding PDF can be written as $f_I(x) = \frac{1}{x\gamma} f_r\Big((\frac{x}{C})^{-\frac{1}{\gamma}}\Big)(\frac{x}{C})^{\frac{-1}{\gamma}}$. Accordingly, a closed-form expression for the MGF of the interference I can be formulated as $M_I(t) = \int_0^\infty e^{-tx} f_I(x) dx$. Note that the same steps apply for the derivation of the MGF of the signal of interest ($M_S(t)$).

Denote by I_{tot} the cumulative interference from the macro cell (I_m) and the small cells (I_i), at the reference small cell. Consequently, I_{tot} can be written as: $I_{tot} = I_m + I_i$. Considering I_m and I_i as independent variables, the MGF of the cumulative interference I_{tot} can be calculated as follows: $M_{I_{tot}}(t) = M_{I_m}(t) M_{I_i}(t)$.

Based on the MGF expressions derived for S and I_{tot}, the average capacity per unit bandwidth can be calculated using the lemma proposed in [33] as follows:

$C = \mathbb{E}[\ln(1+\frac{S}{I_{tot}+\sigma^2})] = \int_0^\infty \frac{M_{I_{tot}}(t) - M_S(t) M_{I_{tot}}(t)}{t} e^{-(\sigma^2)t} dt$

$= \int_0^\infty \frac{M_{I_m}(t) M_{I_i}(t) - M_S(t) M_{I_m}(t) M_{I_i}(t)}{t e^{-at}} e^{-(\sigma^2+a)t} dt.$

This expression can be solved efficiently by expressing it in terms of the weights w_e and abscissas x_e of a Laguerre orthogonal polynomial as follows:

$$C = \sum_{e=1}^{n} w_e \Big(\frac{M_{I_m}(x_e/(\sigma^2+a)) M_{I_i}(x_e/(\sigma^2+a))}{x_e e^{-(a x_e)/(\sigma^2+a)}} - \frac{M_S(x_e/(\sigma^2+a)) M_{I_m}(x_e/(\sigma^2+a)) M_{I_i}(x_e/(\sigma^2+a))}{x_e e^{-(a x_e)/(\sigma^2+a)}} \Big).$$

In this work, the a parameter was introduced to resolve the scaling problem in Laguerre polynomial, more specifically in the $M(t)$ expression. Adding the a parameter will ensure scalable values of the MGF function with $M(x_e/(\sigma^2+a))$. a is set to 10^{-4} in the scenarios where the macro cell is in a DL mode and to 10^{-6} in the scenarios where the macro cell is in an UL mode.

Special Case: $\psi = \{s, m\}$, *i.e.* $N_s = 1$ *and* $I_i = 0$: In case of a network consisting of one macro cell and one reference small cell, the latter will be purely affected by the macro cell interferer and therefore $I_{tot} = I_m = I$. Accordingly, the capacity expression can be formulated as follows:

$$C = \sum_{e=1}^{n} w_e \Big(\frac{M_I(x_e/(\sigma^2+a))}{x_e e^{-(a x_e)/(\sigma^2+a)}} - \frac{M_S(x_e/(\sigma^2+a)) M_I(x_e/(\sigma^2+a))}{x_e e^{-(a x_e)/(\sigma^2+a)}} \Big).$$

Remark 2 (Uplink Power Control): Uplink power control can also be added to the developed model. Based on the open-loop power control strategy standardized in 3GPP LTE [34], the transmit power of a mobile user is given by:

$$P_t = min(P_{max}, P_0 r_s^\gamma),$$

where r_s is the distance of a user from its serving BS (macro BS or small cell BS), P_0 is the desired received signal level at the BS and P_{max} denotes the maximum transmit power capability per user. Consequently, the uplink signal power received at the reference BS with power control can be given as $S = KP_t r_s^{-\gamma}$ with:

$$S = \begin{cases} KP_0, & P_{max} > P_0 r_s^\gamma \\ KP_{max} r_s^{-\gamma}, & P_{max} \leq P_0 r_s^\gamma, \end{cases}$$

and the interference caused at a reference BS (or user) from a given small cell (or macro cell) interferer, can then be derived as $I = KP_t r_i^{-\gamma}$ with:

$$I = \begin{cases} KP_0 r_s^\gamma r_i^{-\gamma}, & P_{max} > P_0 r_s^\gamma \\ KP_{max} r_i^{-\gamma}, & P_{max} \leq P_0 r_s^\gamma, \end{cases}$$

where r_i is distance from the interferer to the reference BS (or user). The PDF of I can be derived by averaging over r_s the PDF of $f_{r_i}(r)_{|r_s}$.

It is important to note that the power control mechanism leads in average to reduction in power consumption when a user in a specific position is able to compensate the overall path loss with $P_0 r_s^\gamma < P_{max}$. In this case, average reduction in power consumption (PR) can be defined as: $PR = \mathbb{E}[P_{max} - P_0 r_s^\gamma]$.

Simulation results showing the impact of power control on the system throughput and the network power consumption, will be discussed under Section 6.3.1.

Remark 3 (Unsynchronized TDD Configuration): Although in this work the model is developed based on a synchronized TDD configuration assumption across small cells, it can be well adapted to consider an unsynchronized TDD configuration by deriving two additional expressions for the co-tier interference experienced from the interfering small cell at the reference small cell:

1) In the case where the interfering small cell operates in uplink and the reference small cell operates in downlink, the PDF of the distance from the interfering small cell user to the reference small cell user (u_{is}) can be derived similarly to the PDF of u_{ms} in (3):

$$f_{u_{is}}(r) = \int_{r-R_s}^{r+R_s} f_{u_{is}}(r)_{|r_{si}} f_{r_{si}}(r_{si}) dr_{si},$$

This article has been accepted for publication in a future issue of this journal, but has not been fully edited. Content may change prior to final publication. Citation information: DOI 10.1109/TMC.2020.2979447, IEEE Transactions on Mobile Computing

where $f_{u_{is}}(r)_{|r_{si}} = \frac{1}{\pi R_s^2}(\pi r - 2r\arcsin(\frac{r_{si}^2+r^2-R_s^2}{2r_{si}r}))$ and $f_{r_{si}}(r_{si})$ defined as follows:

$$f_{r_{si}}(r_{si}) = \frac{1}{\pi R_s^2}\Big(\pi r_{si} - 2r_{si}\arcsin(\frac{d_{12}^2 + r_{si}^2 - R_s^2}{2d_{12}r_{si}})\Big),$$

2) In the case where the interfering small cell operates in downlink and the reference small cell operates in uplink, the distance from the interfering small cell to the reference small cell is constant and equal to d_{12}.

Note that slight changes to the interference's expressions at the expanded area are applied as well depending on both the user association criteria and the macro cell transmission direction (whether UL or DL). Simulation results showing the impact of considering an unsynchronized TDD configuration, will be discussed under Section 6.3.2.

4 Impact of the Decoupling Access on a TDD HetNet

In this section, ψ is set to $\{s, m\}$, i.e. a HetNet consisting of one small cell s and one macro cell m. We consider this model to study the benefits that the decoupling access mode can bring to a HetNet TDD basic system. The section that follows, will assess the benefit of decoupling in a more complex environment where multiple small cells are deployed. Introducing the DUDA mode necessitates a thorough comparison study with the conventional CUDA mode. We first derive the statistics of the interference signal and the downlink/uplink received power of both DUDA and CUDA modes and then analyze the system performance of these two access modes. The main performance metric that is being measured, in both UL and DL, is the average capacity per unit bandwidth i.e. the average spectral efficiency (C_{es}). It is calculated based on the average users capacity in the small cell area added to the average users capacity in the expanded area. Both throughputs have been evaluated and averaged over the period of a defined TDD frame. The average user capacity in each area is derived based on Proposition 1.

For further analysis and to ensure the generality of our study, the CUDA scenario is analyzed by taking into account two cases (Fig. 3):

1) Coupled access in UL and DL with the macro cell.
2) Coupled access in UL and DL with the small cell.

Two cases, as well, can be part of the DUDA mode (Fig. 4):

1) Decoupling strategy where users are associated in UL with the small cell and in DL with the macro cell.
2) Reverse Decoupling strategy where users are associated in UL with the macro cell and in DL with the small cell.

All proposed association strategies (coupled or decoupled), will be compared to the coupled with macro cell case since initially and before applying any change to the network configuration, users in the expanded area are considered in DL and UL as associated with the macro cell.

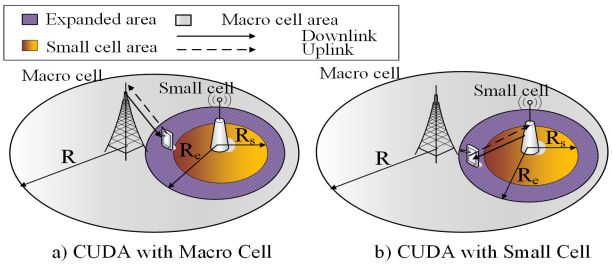

Fig. 3. CUDA illustration.

4.1 Analytical Evaluation of CUDA

4.1.1 CUDA with Macro Cell

In each of the below possible UL/DL combinations, we derive the statistics of both the small cell and the expanded area users.

a) Down - Down Mode: The downlink interference from the small cell BS to the mobile user in the expanded area is defined as $I_e = KP_s r_e^{-\gamma}$, with r_e the distance of the user in the expanded area from the small cell BS. Since we consider uniformly distributed users, the distribution of the distance r_e of users in the expanded area bounded by R_s and R_e is given by:

$$f_{r_e}(r) = \frac{2r}{R_e^2 - R_s^2}, \quad R_s \leq r \leq R_e. \tag{16}$$

The downlink received power by the mobile user in the expanded area is defined as $S_e = KP_m r_{me}^{-\gamma}$ with r_{me} the distance of the user in the expanded area from the macro cell BS. Based on [29], the PDF of r_{me} can be written as:

$$f_{r_{me}}(r) = \begin{cases} \frac{f(r)}{(\pi R_e^2 - \pi R_s^2)}, & d - R_e \leq r \leq d - R_s \\ \frac{f(r) - g(r)}{(\pi R_e^2 - \pi R_s^2)}, & d - R_s \leq r \leq d + R_s \\ \frac{f(r)}{(\pi R_e^2 - \pi R_s^2)}, & d + R_s \leq r \leq d + R_e, \end{cases} \tag{17}$$

where $f(r) = \pi r - 2r\arcsin(\frac{d^2+r^2-R_e^2}{2dr})$ and $g(r) = \pi r - 2r\arcsin(\frac{d^2+r^2-R_s^2}{2dr})$.

As for the statistics related to the small cell users, the downlink interference from the macro BS to the small cell users is defined as $I_s = KP_m r_{ms}^{-\gamma}$ with r_{ms} the distance of the macro BS from the small cell user. Based on [28], the PDF of r_{ms} can be obtained as a result of the cell intersection with the circle of radius R_s:

$$f_{r_{ms}}(r) = \frac{1}{\pi R_s^2}\Big(\pi r - 2r\arcsin(\frac{d^2 + r^2 - R_s^2}{2dr})\Big). \tag{18}$$

The downlink received power by the small cell user is defined as $S_s = KP_s r_s^{-\gamma}$ with r_s the distance of the small cell user from the small cell BS. Since we consider uniformly distributed users, the distribution of the distance r_s of a small cell user is given by:

$$f_{r_s}(r) = \frac{2r}{R_s^2}, \quad 0 \leq r \leq R_s. \tag{19}$$

Note that the same expressions of S_s and r_s apply when tackling the small cell user's statistics in all coming scenarios, where the transmit power varies depending on the link direction, either UL or DL.

b) Up - Down Mode: The uplink interference from the small cell BS to the macro BS is defined as $I_e = KP_s d^{-\gamma}$ with d the distance of small cell BS from the macro cell BS. The uplink desired signal of the mobile user in the expanded area is defined as $S_e = KP_{um} r_{me}^{-\gamma}$. The PDF of r_{me} can be given by iterating the same analysis as in (17).

As for the statistics related to the small cell users, the downlink interference from the macro cell user to the small cell user is defined as $I_s = KP_{um} u_{ms}^{-\gamma}$. The PDF of u_{ms} is derived by averaging over the PDF of r_{sm} ($f_{r_{sm}}(r_{sm})$):

$$f_{u_{ms}}(r) = \int_{r-R_s}^{r+R_s} f_{u_{ms}}(r)_{|r_{sm}} f_{r_{sm}}(r_{sm}) dr_{sm}, \tag{20}$$

where $f_{u_{ms}}(r)_{|r_{sm}}$ can be derived as follows:

$$f_{u_{ms}}(r)_{|r_{sm}} = \frac{1}{\pi R_s^2}(\pi r - 2r \arcsin(\frac{r_{sm}^2 + r^2 - R_s^2}{2 r_{sm} r})).$$

As for the derivation of the r_{sm} statistics, and since $R > d$, two cases must be taken into account based on [28]:

$$f_{r_{sm}}(r_{sm}) = \begin{cases} \frac{2\pi r_{sm}}{\pi R^2 - \pi R_s^2}, & R_s \leq r_{sm} < R - d \\ k(r_{sm}), & R - d \leq r_{sm} \leq R + d, \end{cases} \tag{21}$$

$k(r_{sm}) = \frac{1}{\pi R^2 - \pi R_s^2}(\pi r_{sm} - 2 r_{sm} \arcsin(\frac{d^2 + r_{sm}^2 - R^2}{2 d r_{sm}}))$.

c) Up - Up Mode: The uplink interference from the small cell user to the macro BS is defined as $I_e = KP_{us} r_{ms}^{-\gamma}$. The PDF of r_{ms} is given by (18). The uplink signal of the mobile user in the expanded area is defined as $S_e = KP_{um} r_{me}^{-\gamma}$. The PDF of r_{me} can be defined similarly as in (17).

As for the statistics related to the small cell users, the uplink interference from the macro cell user to the small cell BS is defined as $I_s = KP_{um} r_{sm}^{-\gamma}$. The PDF of r_{sm} is defined similarly as in (21).

d) Down - Up Mode: The downlink interference from the small cell user BS to the mobile user in the expanded area is defined as $I_e = KP_{us} r_{es}^{-\gamma}$ with r_{es} the distance of the user in the expanded area from the small cell user.
The PDF of r_{es} can be derived using the closed-form expression obtained in [29]:

$$f_{r_{es}}(r) = \begin{cases} \frac{2r}{b^2}, & 0 \leq r \leq b - a \\ \frac{r}{\pi}\Big(\frac{2v(r) - \sin(2v(r))}{b^2} + \\ \frac{2w(r) - \sin(2w(r))}{a^2}\Big), & b - a \leq r \leq b + a, \end{cases} \tag{22}$$

where $a = R_s$, $b = R_e$, $v(r) = \arccos(\frac{r^2 - b^2 + a^2}{2ra})$ and $w(r) = \arccos(\frac{r^2 + b^2 - a^2}{2rb})$.
The downlink received power by the mobile user in the expanded area is defined as $S_e = KP_m r_{me}^{-\gamma}$. Repeating the same analysis as in (17), we can define the PDF of r_{me}.

As for the statistics related to the small cell users, $I_s = KP_m d^{-\gamma}$ and $S_s = KP_{us} r_s^{-\gamma}$.

4.1.2 CUDA with Small Cell

a) Down - Down Mode: The downlink interference from the macro BS to the mobile user in the expanded area is defined as $I_e = KP_m r_{me}^{-\gamma}$. The PDF of r_{me} is given by (17). The downlink received power by the mobile user in the expanded area is defined as $S_e = KP_s r_e^{-\gamma}$. The distribution of r_e is given by (16).

As for the statistics related to the small cell users, the downlink interference from the macro BS to the small cell users is defined as $I_s = KP_m r_{ms}^{-\gamma}$. The PDF of r_{ms} is given by (18).

b) Up - Down Mode: The downlink interference from the macro cell user to the small cell user that is located inside the area bounded by R_e, is defined as $I_e = KP_{um} u_{me}^{-\gamma}$. The PDF of u_{me} is given by replacing R_s with R_e in (20):

$$f_{u_{me}}(r) = \int_{r-R_e}^{r+R_e} f_{u_{me}}(r)_{|r_{sm}} f_{r_{sm}}(r_{sm}) dr_{sm}, \tag{23}$$

where $f_{u_{me}}(r)_{|r_{sm}} = \frac{1}{\pi R_e^2}(\pi r - 2r \arcsin(\frac{r_{sm}^2 + r^2 - R_e^2}{2 r_{sm} r}))$ and $f_{r_{sm}}(r_{sm})$ is formulated as:

$$f_{r_{sm}}(r_{sm}) = \begin{cases} \frac{2\pi r_{sm}}{\pi R^2 - \pi R_e^2}, & R_e \leq r_{sm} < R - d \\ s(r_{sm}), & R - d \leq r_{sm} \leq R + d, \end{cases} \tag{24}$$

with $s(r_{sm}) = \frac{1}{\pi R^2 - \pi R_e^2}(\pi r_{sm} - 2 r_{sm} \arcsin(\frac{d^2 + r_{sm}^2 - R^2}{2 d r_{sm}}))$.
The downlink received power by the mobile user in the expanded area is defined as $S_e = KP_s r_e^{-\gamma}$. The distribution of r_e is given by (16).

As for the statistics related to the small cell users, the downlink interference from the macro cell user to the small cell user that is located inside the area bounded by R_e, is defined as $I_s = KP_{um} u_{ms}^{-\gamma}$. The distribution of u_{ms} is given by (23). For simplicity, we consider that the distance from the macro user to either the small cell user or the user in the expanded area is the same and denoted by u_{ms}. This approximation is acceptable since small cells are notably smaller than macro cells.

c) Up - Up Mode: The uplink interference from the macro cell user that is located outside the area bounded by R_e to the small cell BS, is defined as $I_e = KP_{um} r_{sm}^{-\gamma}$. The PDF of r_{sm} is derived as in (24) where R_e replaces R_s.

As for the statistics related to the small cell users, the uplink interference is considered as $I_s = KP_{um} r_{sm}^{-\gamma}$. The same distance r_{sm} as in (24) will be studied for simplicity. The accuracy of this approximation will be validated in the next sections using Monte-Carlo simulations.

d) Down - Up Mode: The uplink interference from the macro cell BS to the small cell BS is defined as $I_e = KP_m d^{-\gamma}$ and the desired signal as $S_e = KP_{us} r_e^{-\gamma}$. The distribution of r_e is given by (16).

As for the statistics related to the small cell users, they can be modeled by replacing r_e with r_s in the aforementioned expressions derived for the mobile users in the expanded area.

4.2 Analytical Evaluation of DUDA

4.2.1 DUDA with Decoupling

a) Down - Down Mode: In this scenario, the same expressions will be derived as in the Down - Down scenario defined for the CUDA with the macro cell case.

b) Up - Down Mode: In this scenario, users with a decoupled access will be in silent mode. Consequently, the average throughput for users in the expanded area will not be considered.

As for the statistics related to the small cell users, the downlink interference from the macro cell user to the small cell user that is located inside the area bounded by R_e, is

This article has been accepted for publication in a future issue of this journal, but has not been fully edited. Content may change prior to final publication. Citation information: DOI 10.1109/TMC.2020.2979447, IEEE Transactions on Mobile Computing

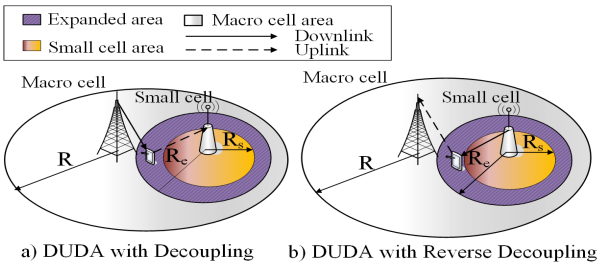

Fig. 4. DUDA illustration.

defined as $I_s = KP_{um}u_{ms}^{-\gamma}$.
The distribution of u_{ms} is given by (23) where R_e replaces R_s.

c) Up - Up Mode: In this scenario, the same expressions will be derived as in the Up - Up scenario defined for the CUDA with the small cell case.

d) Down - Up Mode: In this scenario, users in the expanded area can operate at the same time in uplink and downlink. The downlink interference from the small cell user to the mobile user in the expanded area is defined as $I_e = KP_{us}r_{es}^{-\gamma}$. The PDF of r_{es} is given by (22).
The downlink desired signal of the user in the expanded area is defined as $S_e = KP_m r_{me}^{-\gamma}$. The PDF of r_{me} is given by (17). As for the uplink transmission, the interference from the macro BS to the small cell BS is defined as $I_e = KP_m d^{-\gamma}$ and the uplink desired signal as $S_e = KP_{us}r_s^{-\gamma}$.

As for the statistics related to the small cell users, $I_s = KP_m d^{-\gamma}$ and $S_s = KP_{us}r_s^{-\gamma}$.

4.2.2 DUDA with Reverse Decoupling

a) Down - Down Mode: In this scenario, the same expressions will be derived as in the Down - Down scenario defined for the CUDA with the small cell case.

b) Up - Down Mode: In this scenario, users in the expanded area can operate at the same time in uplink and downlink. The downlink interference from the macro cell user to the small cell user that is located inside the area bounded by R_e, is defined as $I_e = KP_{um}u_{me}^{-\gamma}$.
The PDF of u_{me} is given by (23). The downlink desired signal of the user in the expanded area is defined as $S_e = KP_s r_e^{-\gamma}$. The uplink interference from the small cell BS to the macro BS is defined as $I_e = KP_s d^{-\gamma}$ and the uplink desired signal as $S_e = KP_{um}r_{me}^{-\gamma}$.

As for the statistics related to the small cell users, the downlink interference from the macro cell user to the small cell user that is located inside the area bounded by R_e, is defined as $I_s = KP_{um}u_{ms}^{-\gamma}$.
For simplicity, we consider that the distance of the macro user from either the small cell user or the user in the expanded area is approximately the same and denoted by u_{ms}. This approximation is valid due to the notably smaller size of small cells in comparison with the macro cell.

c) Up - Up Mode: In this scenario, the same expressions will be derived as in the Up - Up scenario defined for the CUDA with the macro cell case.

d) Down - Up Mode: In this scenario, users with a reversed decoupled access will be in silent mode. Consequently, the average throughput for users in the expanded area will not be considered.

As for the statistics related to the small cell users, $I_s = KP_m d^{-\gamma}$ and $S_s = KP_{us}r_s^{-\gamma}$.

5 Decoupling Gain Analysis in Multiple Small Cells Environment

It has been proven that the decoupling strategy maintains a higher throughput in UL and DL in comparison with other association policies in TDD HetNet with a single small cell [29]. The latter result remains valid in the case of multiple small cells deployment where all association policies are facing approximately the same degradation in throughput due to the co-tier interference inflected by interfering small cells. In this context, this section focuses on the analytical evaluation of the decoupling gain brought in UL and DL, that depends mainly on the distance between small cells.

The decoupling gain, denoted as η_i, is defined as the ratio between the throughput achieved when decoupling is adopted and the throughput achieved without decoupling (in the coupled with macro (CM) case):

$$\eta_i = \frac{Throughput_i(\text{Decoupling}) - Throughput_i(\text{CM})}{Throughput_i(\text{CM})}, \quad (25)$$

where $i \in \{UL, DL\}$.
To analyze the decoupling gain in a multiple small cells TDD HetNet, it is important to develop a complete model for both the CM and the decoupling cases. Moreover, calculating the decoupling gain in one direction (UL or DL) necessitates measuring C_{es} in that direction for both cases. C_{es} is computed by adding the average users capacity in the small cell area (C_s) to the average users capacity in the expanded area (C_e).

5.1 Uplink Decoupling gain

In the Down - Up and Up - Up scenarios, small cell users along with the users in the expanded area are operating in uplink. Hence, the latter two scenarios present a considerable part of the overall uplink capacity (C_{es}), whereas the Up - Down case considers a negligible part ($C_{es} = C_e \simeq 0$).

5.1.1 Down - Up Scenario

a) CM Case: For the C_s calculation, closed-form expressions are derived for:

- $I_m = KP_m d$.
- $I_i = KP_{us}r_{si}$, where $d_{12} - R_s \leq r_{si} \leq d_{12} + R_s$.
- $S_s = KP_{us}r_s$, where $0 \leq r_s \leq R_s$.

The PDF $f_{r_{si}}(r)$ is given by (16), an expression derived in the case of two small cells:

$$f_{r_{si}}(r) = \frac{1}{\pi R_s^2}\Big(\pi r - 2r\arcsin(\frac{d_{12}^2 + r^2 - R_s^2}{2d_{12}r})\Big). \quad (26)$$

In this case, $C_e = 0$.

b) Decoupling Case: For the C_s calculation, closed-form expressions are derived for:

- $I_m = KP_m d$.
- $I_i = KP_{us}r_{si}$, where $d_{12} - R_e \leq r_{si} \leq d_{12} + R_e$.
- $S_s = KP_{us}r_s$, where $0 \leq r_s \leq R_s$.

The PDF $f_{r_{si}}(r)$ is given by replacing R_s with R_e in (26):

$$f_{r_{si}}(r) = \frac{1}{\pi R_e^2}\Big(\pi r - 2r\arcsin(\frac{d_{12}^2 + r^2 - R_e^2}{2d_{12}r})\Big). \quad (27)$$

The same interference expressions will be derived for the calculation of C_e. However, S_e is defined as: $S_e = KP_{us}r_e$, where $R_s \leq r_e \leq R_e$.

5.1.2 Up - Up Scenario

a) CM Case: For the C_s calculation, closed-form expressions are derived for:

- $I_m = KP_{um}r_{sm}$, where $R_s \leq r_{sm} \leq R + d$.
- $I_i = KP_{us}r_{si}$, where $d_{12} - R_s \leq r_{si} \leq d_{12} + R_s$.
- $S_s = KP_{us}r_s$, where $0 \leq r_s \leq R_s$.

The PDF of r_{sm} is derived as follows:

$$f_{r_{sm}}(r) = \begin{cases} \frac{2\pi r}{(\pi R^2 - 2\pi R_s^2)}, & R_s \leq r < R - d \\ \frac{f(r)}{(\pi R^2 - 2\pi R_s^2)}, & R - d \leq r \leq d_{12} - R_s \\ \frac{f(r) - g(r)}{(\pi R^2 - 2\pi R_s^2)}, & d_{12} - R_s \leq r \leq d_{12} + R_s \\ \frac{f(r)}{(\pi R^2 - 2\pi R_s^2)}, & d_{12} + R_s \leq r \leq R + d, \end{cases} \quad (28)$$

where $f(r) = \pi r - 2r\arcsin(\frac{d^2 + r^2 - R^2}{2dr})$ and $g(r) = \pi r - 2r\arcsin(\frac{d_{12}^2 + r^2 - R_s^2}{2d_{12}r})$.

The PDF of r_{si} is given by (26).
In this case, $C_e \simeq 0$.

b) Decoupling Case: For the C_s calculation, closed-form expressions are derived for:

- $I_m = KP_{um}r_{sm}$, where $R_e \leq r_{sm} \leq R + d$.
- $I_i = KP_{us}r_{si}$, where $d_{12} - R_e \leq r_{si} \leq d_{12} + R_e$.
- $S_s = KP_{us}r_s$, where $0 \leq r_s \leq R_s$.

The PDF $f_{r_{sm}}(r)$ is given by replacing R_s with R_e in (28):

$$f_{r_{sm}}(r) = \begin{cases} \frac{2\pi r}{(\pi R^2 - 2\pi R_e^2)}, & R_e \leq r < R - d \\ \frac{f(r)}{(\pi R^2 - 2\pi R_e^2)}, & R - d \leq r \leq d_{12} - R_e \\ \frac{f(r) - g(r)}{(\pi R^2 - 2\pi R_e^2)}, & d_{12} - R_e \leq r \leq d_{12} + R_e \\ \frac{f(r)}{(\pi R^2 - 2\pi R_e^2)}, & d_{12} + R_e \leq r \leq R + d, \end{cases} \quad (29)$$

where $f(r) = \pi r - 2r\arcsin(\frac{d^2 + r^2 - R^2}{2dr})$ and $g(r) = \pi r - 2r\arcsin(\frac{d_{12}^2 + r^2 - R_e^2}{2d_{12}r})$.

The PDF of r_{si} is given by (27).
The same interference expressions will be derived for the calculation of C_e. However, S_e is defined as: $S_e = KP_{us}r_e$.

5.2 Downlink Decoupling gain

In the Up - Down and Down - Down scenarios, small cell users along with the users in the expanded area are operating in downlink. Hence, the latter two scenarios present a considerable part of the overall downlink capacity (C_{es}), whereas the Down - Up case considers a negligible part ($C_{es} = C_e \simeq 0$).

5.2.1 Up - Down Scenario

a) CM Case: For the C_s calculation, closed-form expressions are derived for:

- $I_m = KP_{um}u_{ms}$, where $0 \leq u_{ms} \leq R + d + R_s$.
- $I_i = KP_sr_{is}$, where $d_{12} - R_s \leq r_{is} \leq d_{12} + R_s$.
- $S_s = KP_sr_s$, where $0 \leq r_s \leq R_s$.

u_{ms} represents the distance from the macro cell user to the small cell user that is located inside the area bounded by R_s. The PDF of u_{ms} is derived by averaging over the PDF of r_{sm} ($f_{r_{sm}}(r_{sm})$):

$$f_{u_{ms}}(r) = \int_{r-R_s}^{r+R_s} f_{u_{ms}}(r)_{|r_{sm}} f_{r_{sm}}(r_{sm}) dr_{sm}, \quad (30)$$

where r_{sm} is the distance of the reference small cell BS from the macro cell user and $f_{u_{ms}}(r)_{|r_{sm}}$ denotes the PDF of u_{ms} conditioned on r_{sm}.
In this case, the expanded areas of both small cells are part of the macro user region and thus, $f_{r_{sm}}$ will be derived using R_s as the main parameter to determine the macro user area boundaries as in (28). Since C_s represents the average capacity of the reference small cell users located inside the area bounded by R_s, the integral of $f_{u_{ms}}(r)_{|r_{sm}}$ will range from $r - R_s$ to $r + R_s$. The PDF $f_{r_{is}}(r)$ is given by (9), an expression derived in the case of two small cells:

$$f_{r_{is}}(r) = \frac{1}{\pi R_s^2}\Big(\pi r - 2r\arcsin(\frac{d_{12}^2 + r^2 - R_s^2}{2d_{12}r})\Big). \quad (31)$$

In the CM case under the Up - Down scenario, $C_e = 0$ and thus, $C_{es} = C_s$.

b) Decoupling Case: For the C_s calculation, closed-form expressions are derived for:

- $I_m = KP_{um}u_{ms}$, where $R_e - R_s \leq u_{ms} \leq R + d + R_s$.
- $I_i = KP_sr_{is}$, where $d_{12} - R_s \leq r_{is} \leq d_{12} + R_s$.
- $S_s = KP_sr_s$, where $0 \leq r_s \leq R_s$.

u_{ms} represents the distance from the macro cell user to the small cell user that is located inside the area bounded by R_s. The PDF of u_{ms} is derived by averaging over the PDF of r_{sm} ($f_{r_{sm}}(r_{sm})$):

$$f_{u_{ms}}(r) = \int_{r-R_s}^{r+R_s} f_{u_{ms}}(r)_{|r_{sm}} f_{r_{sm}}(r_{sm}) dr_{sm}. \quad (32)$$

Contrary to the CM case, the expanded areas of both small cells are out of the macro user region and thus, $f_{r_{sm}}$ will be derived using R_e as the main parameter to determine the macro user area boundaries:

$$f_{r_{sm}}(r) = \begin{cases} \frac{2\pi r}{(\pi R^2 - 2\pi R_e^2)}, & R_e \leq r < R - d \\ \frac{f(r)}{(\pi R^2 - 2\pi R_e^2)}, & R - d \leq r \leq d_{12} - R_e \\ \frac{f(r) - g(r)}{(\pi R^2 - 2\pi R_e^2)}, & d_{12} - R_e \leq r \leq d_{12} + R_e \\ \frac{f(r)}{(\pi R^2 - 2\pi R_e^2)}, & d_{12} + R_e \leq r \leq R + d, \end{cases} \quad (33)$$

where $f(r) = \pi r - 2r\arcsin(\frac{d^2 + r^2 - R^2}{2dr})$ and $g(r) = \pi r - 2r\arcsin(\frac{d_{12}^2 + r^2 - R_e^2}{2d_{12}r})$.

Consequently, u_{ms} will range from $R_e - R_s$ to $R + d + R_s$. Similar to the CM case and since C_s represents the average capacity of the reference small cell users located inside the area bounded by R_s, the integral of $f_{u_{ms}}(r)_{|r_{sm}}$ will range

This article has been accepted for publication in a future issue of this journal, but has not been fully edited. Content may change prior to final publication. Citation information: DOI 10.1109/TMC.2020.2979447, IEEE Transactions on Mobile Computing

from $r - R_s$ to $r + R_s$.
Note that $r_{is}(r)$ follows the same statistical distribution as in the CM case. Whether the user located in the expanded area, is in decoupling or CM state, $r_{is}(r)$ will be reflecting the interference experienced from the interfering small cell BS independently of the small cell user access policy.
In this case, $C_e = 0$ and thus, $C_{es} = C_s$.

5.2.2 Down - Down Scenario

Under this scenario, same expressions are derived for both CM and decoupling cases. Theoretically, it means there is no downlink decoupling gain ($\eta_{DL} = 0$).
For the C_s calculation, closed-form expressions are derived for:

- $I_m = KP_m r_{ms}$, where $d - R_s \leq r_{ms} \leq d + R_s$.
- $I_i = KP_s r_{is}$, where $d_{12} - R_s \leq r_{is} \leq d_{12} + R_s$.
- $S_s = KP_s r_s$, where $0 \leq r_s \leq R_s$.

The PDF of r_{ms} can be obtained as a result of the cell intersection with the circle of radius R_s:

$$f_{r_{ms}}(r) = \frac{1}{\pi R_s^2}\Big(\pi r - 2r \arcsin(\frac{d^2 + r^2 - R_s^2}{2dr})\Big). \quad (34)$$

The PDF of r_{is} is given by (31).
As for the C_e calculation, closed-form expressions are derived for:

- $I_m = KP_m r_{me}$, where $d - R_e \leq r_{me} \leq d + R_e$.
- $I_i = KP_s r_{ie}$, where $d_{12} - R_e \leq r_{ie} \leq d_{12} + R_e$.
- $S_e = KP_s r_e$, where $R_s \leq r_e \leq R_e$.

The PDF of r_{me} can be defined similarly as in (17). As for the distribution of r_{ie} is given by replacing d with d_{12} in (17):

$$f_{r_{ie}}(r) = \begin{cases} \frac{f(r)}{(\pi R_e^2 - \pi R_s^2)}, & d_{12} - R_e \leq r \leq d_{12} - R_s \\ \frac{f(r) - g(r)}{(\pi R_e^2 - \pi R_s^2)}, & d_{12} - R_s \leq r \leq d_{12} + R_s \\ \frac{f(r)}{(\pi R_e^2 - \pi R_s^2)}, & d_{12} + R_s \leq r \leq d_{12} + R_e, \end{cases} \quad (35)$$

where $f(r) = \pi r - 2r \arcsin(\frac{d_{12}^2 + r^2 - R_e^2}{2d_{12}r})$ and $g(r) = \pi r - 2r \arcsin(\frac{d_{12}^2 + r^2 - R_s^2}{2d_{12}r})$.

6 Numerical and Simulation Results

In this section, we first define the system parameters and discuss the Monte-Carlo simulation results that are provided to demonstrate the effectiveness of the derived analytical expressions. The default system parameters are listed in Table 2. We consider frame structures where all uplink/downlink combinations between the macro and small cells are taken into account, as shown in Fig. 5. It is important to note that, relying on this model that encloses all possible inter-link interferences, any other TDD configuration with different length can be easily investigated.

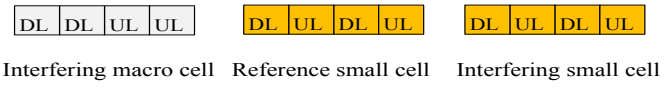

Fig. 5. TDD frame structure in macro and small cells.

TABLE 2
System Parameters

Parameter	Value
Macro cell radius R	1000 m
Small cell radius R_s	200 m
Expanded area radius R_e	300 m
Number of small cells N_s	$1 \leq N_s \leq 2$
Distance between the reference small cell and the macro cell d	600 m
Distance between the reference small cell and the interfering small cell d_{12}	800 m
Path-loss exponent γ	$2 \leq \gamma \leq 3$
Thermal noise power variance σ^2	10^{-12} W/Hz
Macro BS transmission power P_m	20 W
Small cell BS transmission power P_s	0.25 W
Macro user transmission power P_{um}	0.22 W
Small cell user transmission power P_{us}	0.2 W

6.1 TDD HetNet Performance

In order to first evaluate the system performance of a HetNet TDD based system in both uplink and downlink directions, we consider a HetNet with an offset factor $R_e = 0$. C_{es}, in this case, is equivalent to the average user capacity in the reference small cell (C_s). Figure 6 captures the increase in C_s when moving away the reference small cell from the macro cell. The interference, more specifically triggered by the macro BS, reduces when increasing the distance between the small cell and the macro cell. Figure 7 depicts C_s for different values of macro user uplink transmission power. Note that the increase of P_{um} value reduces the average small cell capacity and this is due to the increase of interference triggered mainly by the macro users. Figure 8 investigates the effect of the path loss exponent in order to evaluate the system performance under various propagation conditions and different environments. It can be observed that the increase in path loss exponent enhances the performance of the reference small cell users in uplink and downlink by mitigating the effect of the interference signal.

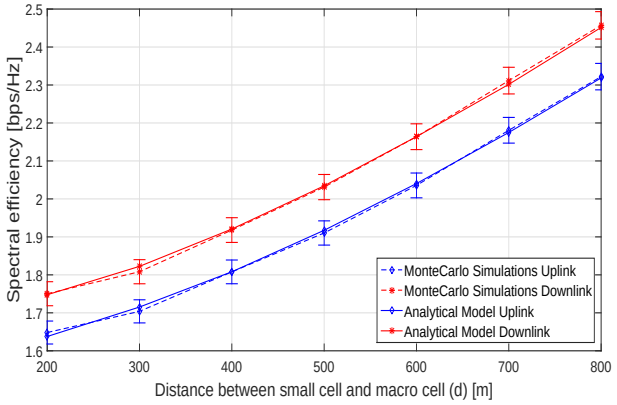

Fig. 6. Capacity per unit bandwidth in the reference small cell as a function of the distance between the reference small cell and the macro cell (d) with $N_s = 1$, $\gamma = 3$ and $P_{um} = 0.22$ W.

This article has been accepted for publication in a future issue of this journal, but has not been fully edited. Content may change prior to final publication. Citation information: DOI 10.1109/TMC.2020.2979447, IEEE Transactions on Mobile Computing

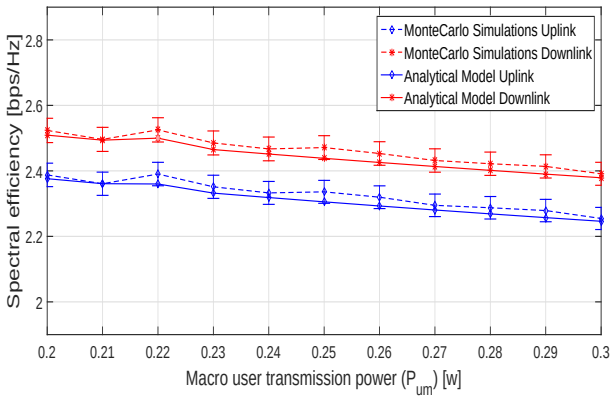

Fig. 7. Capacity per unit bandwidth in the reference small cell as a function of the macro user transmission power (P_{um}) with $N_s = 1$, $\gamma = 3$ and $d = 600$ m.

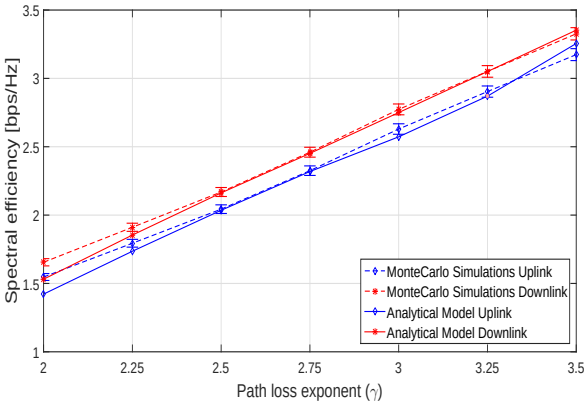

Fig. 8. Capacity per unit bandwidth in the reference small cell as a function of the path loss exponent (γ) with $N_s = 1$, $d = 600$ m and $P_{um} = 0.22$ W.

6.2 Impact of Decoupling Access Policy

Since the CM case represents the current system status before applying any change to the network configuration, our objective is to enhance the performance of the system in downlink and uplink by adopting three different association policies and comparing their performances in terms of spectral efficiency with the CM case.
Figure 9 depicts numerical values of C_{es} for each association strategy and in both UL/DL. We can conclude from this graph that the decoupling case shows an improvement in UL spectral efficiency (SE) around 1.65 bps/Hz in comparison with the CM case where the uplink SE is 1.35 bps/Hz. The same improvement in UL is observed for the coupled access with small cell case. The normal coverage area of the small cell, in this case (coupled with small cell), is expanded and the small cell users along with the users in the expanded area are now connected in UL and DL to the small cell BS. This situation is referred to as cell range expansion (CRE) technique [31]. However and as expected, the coupled access with small cell case or what is called the CRE technique, leads to a degradation in downlink SE which is due mainly to the macro BS downlink interference affecting the users in the CRE region. This harmful downlink interference in the range expansion area is usually solved by applying the Almost Blank Subframe (ABS) technique [32]. This degradation can be easily observed in Fig. 9 where the downlink SE is reduced from 1.94 to 1.74 bps/Hz, whereas the decoupling case is showing a slight DL improvement from 1.94 to 1.96 bps/Hz.

Moving to the reverse decoupling case, we can notice a degradation in SE for both directions, from 1.35 to 1.23 bps/Hz in UL and from 1.94 to 1.78 bps/Hz in DL.
The aforementioned results indicate that the DUDA mode with decoupling access brings greater benefits in the uplink and maintains the same performance improvement in the downlink.

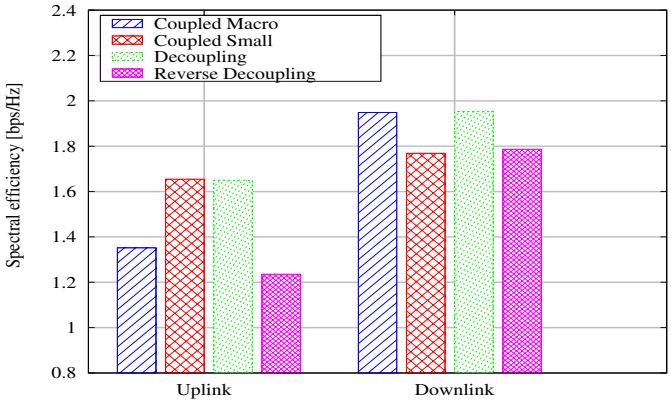

Fig. 9. Capacity per unit bandwidth (C_{es}) in both UL/DL directions for various link association policies with $N_s = 1$, $\gamma = 3$ and $R_e = 300$ m.

Figures 10 and 11 show the uplink and downlink spectral efficiencies, for various association policies while varying R_e, the distance offset factor, between R_s and $R - d$. In both figures, we denote by (Th.) the theoretical results and by (M.C.) the Monte-Carlo simulation results. As expected, the decoupling case among all other cases, maintains a higher SE in uplink and downlink for all offset values. We can observe in Fig. 10 that the uplink SE, for the decoupling case, shows a considerable degradation for R_e values greater than 280 m, whereas the downlink SE, for the same case, shows a continuous improvement for all offset values as shown in Fig. 11. When increasing the offset value, the decoupled users attached to the macro cell in the downlink and to the small cell in the uplink, are now closer to the macro cell and further away from the small cell. Thus, the downlink received power from the macro BS will be effectively increased and the uplink received power by the small cell BS will be decreased. This explains the degradation in uplink SE and the improvement in downlink SE. Consequently, it is paramount to find out the trade-off between the uplink SE and the downlink SE which is in our case a threshold for R_e equal to 260 or 280 m. Last but not least, it can be concluded from Fig. 10 and Fig. 11, that Monte-Carlo simulation results match nearly perfectly the derived capacity expressions for various link association policies.

This article has been accepted for publication in a future issue of this journal, but has not been fully edited. Content may change prior to final publication. Citation information: DOI 10.1109/TMC.2020.2979447, IEEE Transactions on Mobile Computing

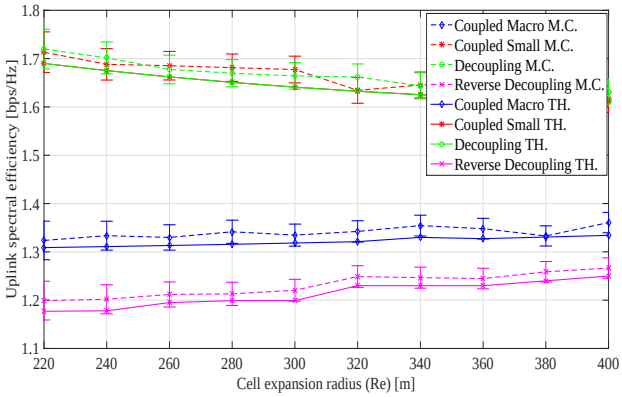

Fig. 10. Comparison of the uplink spectral efficiency between CUDA and DUDA modes for various (R_e) offset factor with $N_s = 1$ and $\gamma = 3$.

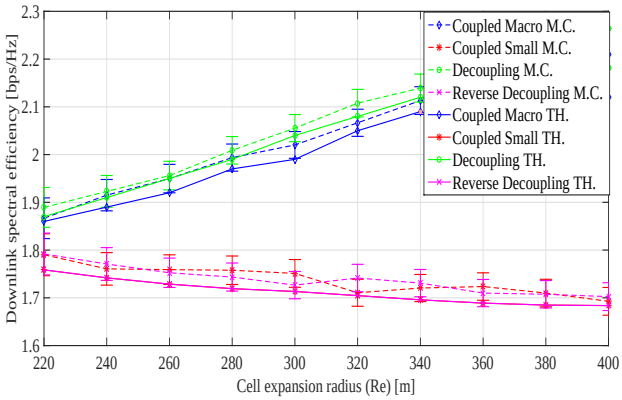

Fig. 11. Comparison of the downlink spectral efficiency between CUDA and DUDA modes for various (R_e) offset factor with $N_s = 1$ and $\gamma = 3$.

6.3 Multiple Small Cells Scenario

A new design parameter emerges when tackling a multiple small cells scenario. This parameter is the distance between small cells denoted by d_{12}. Deploying a new network configuration with randomly positioned interfering small cell implies 1000 iterations of Monte-Carlo simulations to obtain consistent and stable results. For each Monte-Carlo iteration, i.e. for each d_{12}, we generate uniformly distributed users in different cells for a large number of Monte-Carlo simulations (around 1000 iterations), to reach a total of 1 000 000 iterations. Note that the required time to analytically evaluate the decoupling gain expression in (25) is found to be 10 to 15 seconds, giving fairly accurate results with a higher precision ($n = 80$) adopted in the computation of Laguerre polynomial in (15). On the other hand, the computational time for running 1 000 000 Monte-Carlo simulations is given by 4 570 seconds which is significantly larger, when compared to the analytical expression evaluation time. Hence, there is a strong need for an analytical model as a replacement for the time consuming Monte-Carlo simulations, especially in multiple small cells environments. Note that in the derivation of Laguerre expression, the target was first to find the minimal value of n for which the series in (15) converges. It was noticed that, with n=80 and n=100, the expressions converged nearly to the same value with a higher precision. Therefore, n=80 was selected as the minimal value of n that gives accurate and precise results.

In Fig. 12, we evaluate the average user capacity C_{es} in a multiple small cells environment for different association policies. As expected, we notice a decrease in UL and DL throughput values in comparison with the single small cell case (Fig. 9). With the increase in the number of small cells interferers, the interference level increases and thus, the average user throughput decreases for various association policies. Consequently and since the decoupling strategy prevails over the other policies, it will be more interesting to study the impact of the small cells distribution on the decoupling gain in a multiple small cells environment.

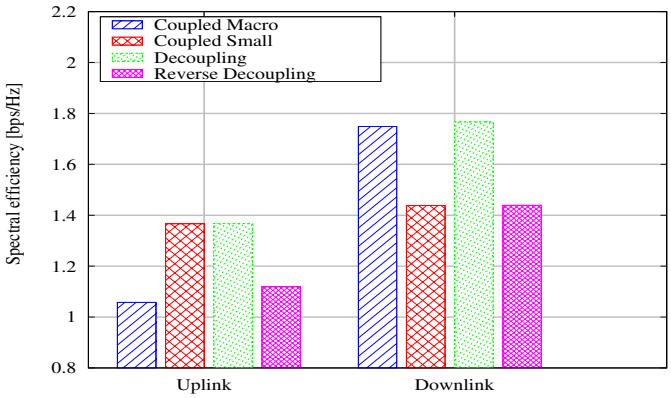

Fig. 12. Capacity per unit bandwidth (C_{es}) in both UL/DL directions for various link association policies with multiple small cells deployment: $N_s = 2$, $\gamma = 3$, $R_e = 300$ m and $d_{12} = 800$ m.

Figure 13 depicts the uplink decoupling gain as a function of the distance between the reference small cell and the interfering small cell (d_{12}). We introduce Monte-Carlo simulations to demonstrate the accuracy of the analytical expressions derived for the decoupling gain in the previous section. We can observe that keeping the interfering small cell far from the reference small cell for a given distance, increases the uplink decoupling gain. Exceeding this threshold, we can notice that the uplink gain maintains a constant value regardless the distance between small cells, i.e. no more gain in UL throughput when moving away the interfering small cell for more than 1100 m from the reference small cell. To better understand this behavior, we benefit from the expressions derived in the previous section for different uplink scenarios (Down - Up and Up - Up), to plot the graph in Fig. 14. Since increasing the distance (d_{12}) has a minimal impact on the uplink gain in the Down - Up scenario, it is clearly shown that the behavior observed in Fig. 13 is provoked mainly by the Up - Up scenario. In the Up - Up scenario and when increasing the distance between small cells to more than 1100 m, the impact of the interfering small user I_i becomes almost negligible and thus, the major impact on the uplink throughput appears to be the interference experienced from the macro user I_m. This interference has a negative impact on the decoupling case in comparison with the CM case, because of the presence of a decoupled zone in the interfering small cell. The latter allows a more closer area for the macro users toward the

This article has been accepted for publication in a future issue of this journal, but has not been fully edited. Content may change prior to final publication. Citation information: DOI 10.1109/TMC.2020.2979447, IEEE Transactions on Mobile Computing

reference small cell and thus, a considerable interference with the uplink desired signal in that small cell. This will explain the steadiness of the uplink gain beyond a given distance (d_{12}).

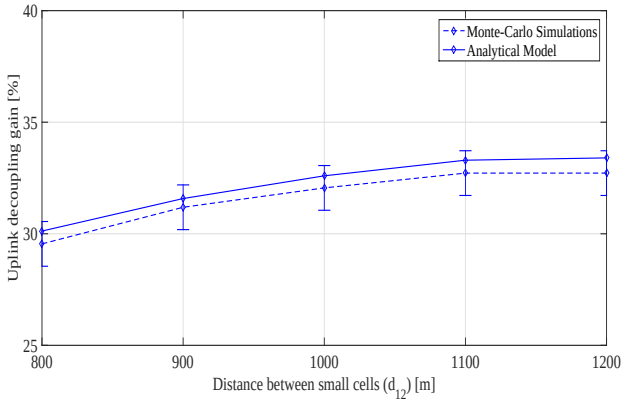

Fig. 13. Uplink decoupling gain (η_{UL}) as a function of the distance between small cells (d_{12}) with $N_s = 2$, $\gamma = 3$ and $R_e = 300$ m.

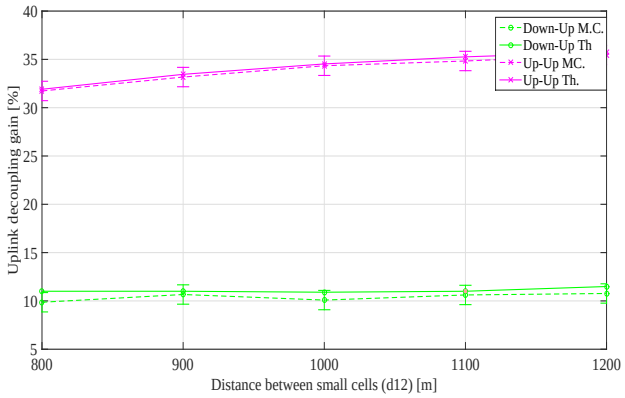

Fig. 14. Uplink decoupling gain breakdown analysis: Down - Up and Up - Up scenarios with $N_s = 2$, $\gamma = 3$ and $R_e = 300$ m.

Figure 15 depicts the downlink decoupling gain as a function of the distance between the reference small cell and the interfering small cell (d_{12}). It can be noticed that the downlink decoupling gain shows a slight downward trend when the distance d_{12} increases. Analyzing the two main downlink scenarios in Fig. 16, we found out that the main reason behind the downlink gain decrease is the interference experienced from the macro user at the small cell user in the Up - Down scenario. Similar to the uplink case, this interference has a negative impact on the decoupling case because of the presence of a decoupled zone in the interfering small cell. The latter allows a more closer area for the macro users to interfere with the downlink desired signal at the small cell user. However, the fact that the decoupling case improves the uplink scenarios in the expanded area at the expense of the downlink scenarios, explains the steadiness of the uplink decoupling gain and the degradation of the downlink gain after a given value of d_{12}. This will explain as well the zero value of the downlink gain obtained in the Down - Down scenario ($\eta_{DL} = 0$).

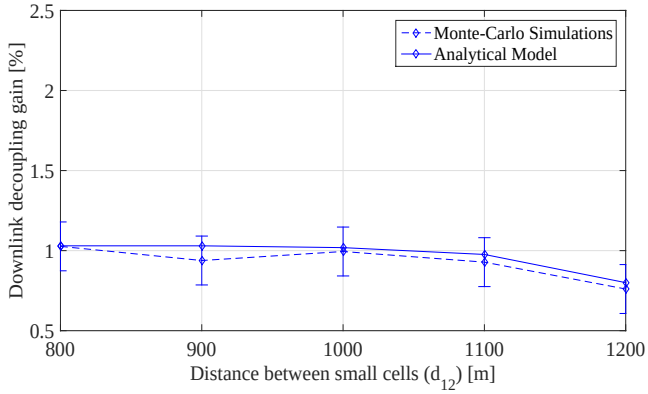

Fig. 15. Downlink decoupling gain (η_{DL}) as a function of the distance between small cells (d_{12}) with $N_s = 2$, $\gamma = 3$ and $R_e = 300$ m.

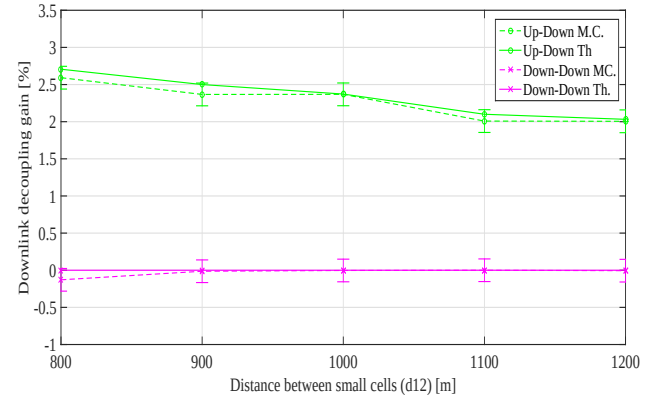

Fig. 16. Downlink decoupling gain breakdown analysis: Up - Down and Down - Down scenarios with $N_s = 2$, $\gamma = 3$ and $R_e = 300$ m.

Furthermore, it would be interesting to address a joint optimization problem, i.e. to evaluate the uplink decoupling gain as a function of two variables: the small cell offset factor and the distance between small cells. While accounting for two small cell offset values ($R_e = 250$ m and $R_e = 300$ m), Fig. 17 highlights the gain obtained for d_{12} below 1100 m, the range where the uplink gain is achieving a significant improvement (Fig. 13). We can notice that the highest uplink decoupling gain (36.2 %) is achieved with $d_{12} = 1000$ m and $R_e = 250$ m. On the other hand, when increasing the offset value to e.g. $R_e = 300$ m, the decoupled zone in the interfering small cell becomes more larger and macro users more closer to the reference small cell and thus, the interference increases. Moreover, the uplink desired signal decreases because of the small cell users that are now transmitting to a farther cell. Consequently, the uplink gain decreases to 32.5 %.

To further elaborate on the joint optimization subject, Fig. 18 captures the system performance under all possible combinations between the small cell coverage (R_e) and small cell placement (d_{12}). Consequently, it is paramount to find the optimal solution which is in our case, a combination of a decoupling region with a radius R_e equal to 210 m and a small cell placement with a distance d_{12} equal to 1000 m.

This article has been accepted for publication in a future issue of this journal, but has not been fully edited. Content may change prior to final publication. Citation information: DOI 10.1109/TMC.2020.2979447, IEEE Transactions on Mobile Computing

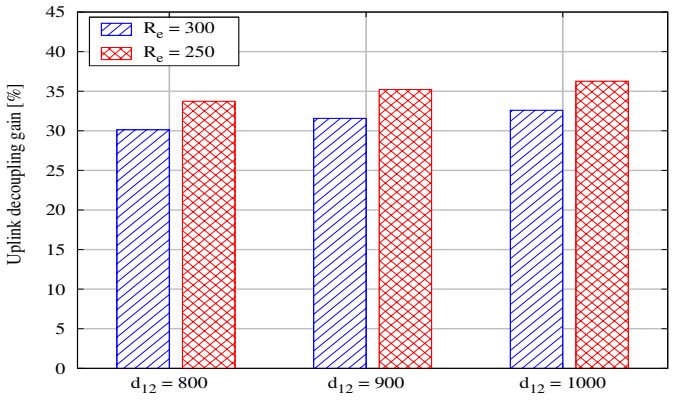

Fig. 17. Uplink decoupling gain (η_{UL}) as a function of both the offset factor (R_e) and the distance between small cells (d_{12}) with $N_s = 2$ and $\gamma = 3$.

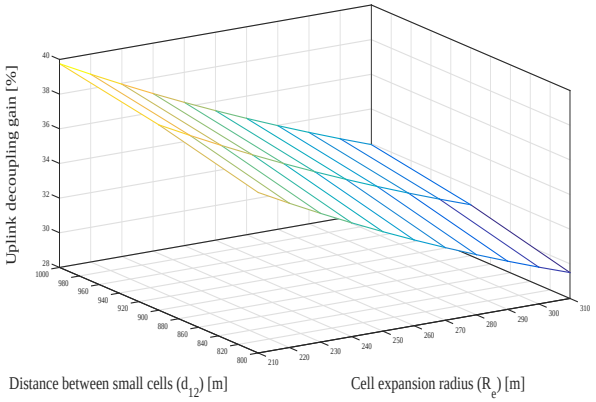

Fig. 18. Uplink decoupling gain (η_{UL}) as a function of all possible (R_e, d_{12}) combinations with $N_s = 2$ and $\gamma = 3$.

6.3.1 Power Control and Reduction in Power Consumption

In order to investigate the impact of considering the power control in our model, we have introduced a power control mechanism with $P_0 = 10^{-7}$ W (-40 dBm) and P_{max} equal to 0.22 W and 0.2 W for macro and small cell users respectively. Comparing Fig. 19 (with power control) to Fig. 12 (without power control), we can deduce that, considering power control (PC) will reduce uplink throughputs and increase downlink throughputs for various association policies. In uplink, considering the PC will reduce the uplink transmitted signal with a slight change in the interference signal; this will explain the decrease in throughput value. However, in downlink, the decrease in uplink transmitted signal will reduce the uplink to downlink interference and keep the same downlink signal; this will justify the increase in downlink throughput. Moreover, it can be concluded that the impact of decoupling remains the same when considering the power control mechanism; the decoupling technique continues to prove that it prevails over the other association policies. Figure 20 shows the reduction in uplink power consumption when implementing the power control mechanism with various association policies. It can be noticed that the coupled with macro cell policy captures the highest reduction in power consumption (PR = 61.7 %), from 0.26 W (without PC) to 0.16 W (with PC). With PC, the macro

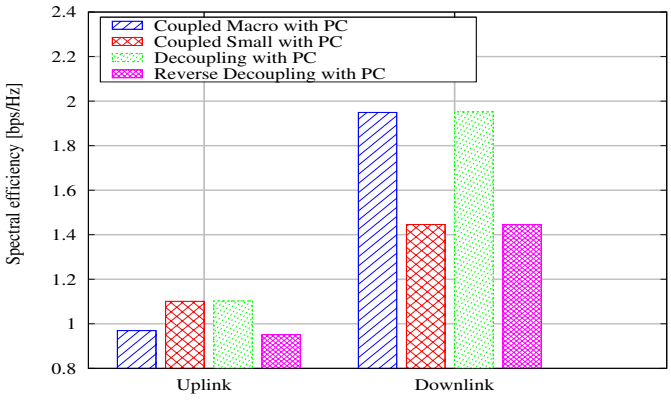

Fig. 19. Spectral efficiency (C_{es}) in both UL/DL directions considering power control (PC) with $P_0 = 10^{-7}$ W (-40 dBm), $N_s = 2$, $\gamma = 3$, $R_e = 300$ m and $d_{12} = 800$ m.

users that are close to their BS refrain from transmitting with P_{max}, instead they will be compensating the path loss with a transmitted power less than P_{max}. This is behind the remarkable uplink power reduction noticed in the coupled with macro case.

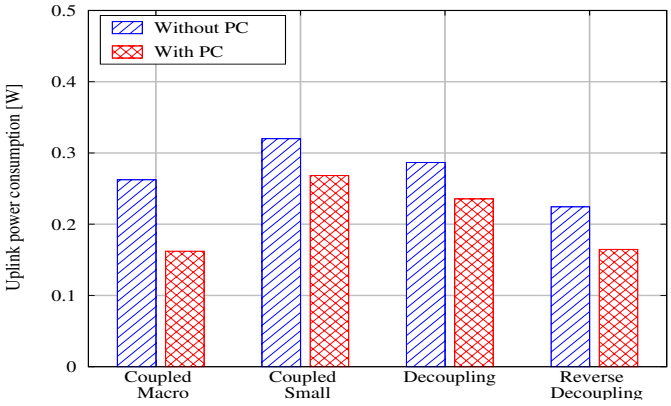

Fig. 20. Uplink power consumption with PC and without PC with $P_0 = 10^{-7}$ W (-40 dBm), $N_s = 2$, $\gamma = 3$, $R_e = 300$ m and $d_{12} = 800$ m.

6.3.2 Unsynchronized TDD configuration

To investigate an unsynchronized case, we consider frame structures that cover all possible uplink/downlink combinations between the macro and the small cells, as shown in Fig. 21. In Fig. 22, a slight decrease in uplink

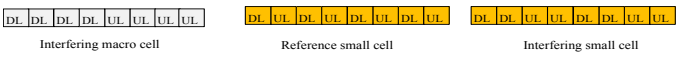

Fig. 21. Unsynchronized TDD frame structure across small cells.

throughput can be noticed for different association policies when considering the unsynchronized TDD case. This is due mainly to the interference experienced from the interfering small cell downlink signal at the reference small cell uplink desired signal. This type of interference, referred to as Down - Up interference, exists and has a considerable effect in the case of an unsynchronized TDD configuration, more specifically in the case where the interfering small

This article has been accepted for publication in a future issue of this journal, but has not been fully edited. Content may change prior to final publication. Citation information: DOI 10.1109/TMC.2020.2979447, IEEE Transactions on Mobile Computing

cell is operating in uplink and the reference small cell is operating in downlink. Moreover, it is interesting to note

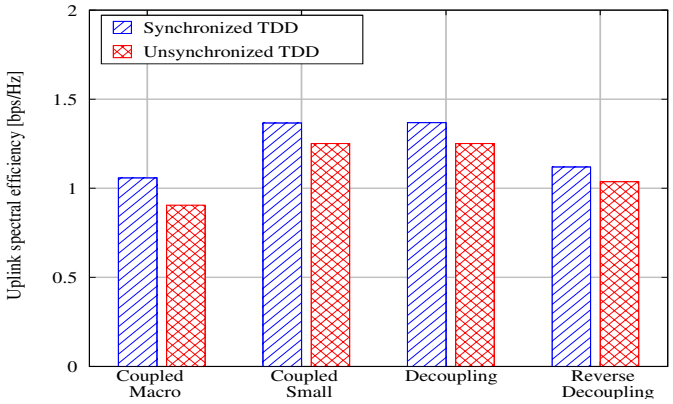

Fig. 22. Comparison of the uplink spectral efficiency (C_{es}) between a synchronized and an unsynchronized TDD mode with $N_s = 2$, $\gamma = 3$, $R_e = 300$ m and $d_{12} = 800$ m.

that, due to the fact that the users in different small cells are not synchronized in downlink/uplink transmissions, users in the expanded areas of the interfering small cell and the reference small cell cannot be decoupled at the same time. Therefore, the decoupling zone at the interfering small cell is no more a second or an additional source of interference. This will explain the improvement brought to the uplink decoupling gain in the case of an unsynchronized TDD configuration as shown in Fig. 23.

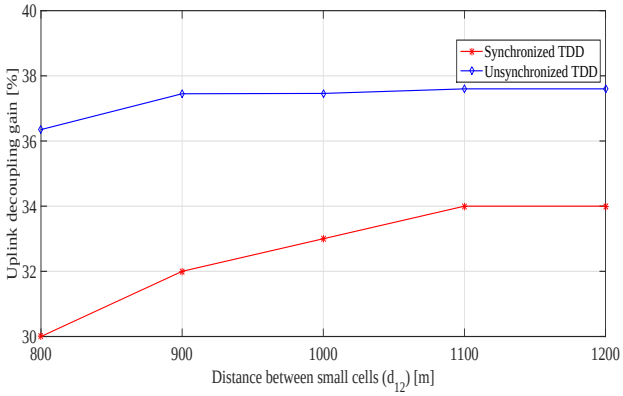

Fig. 23. Comparison of the uplink decoupling gain (η_{UL}) between a synchronized and an unsynchronized TDD mode for various d_{12} values with $N_s = 2$, $\gamma = 3$ and $R_e = 300$ m.

7 Conclusion

We have developed a joint TDD and DUDA statistical model with multiple small cells deployment. This study was based on a geometric probability approach and considered the modeling of both cross-tier and co-tier interferences, in addition to the average user spectral efficiency. First, a performance comparison study for four various cell association rules in TDD HetNet has been conducted. Then we have analyzed, in a multiple small cells environment, the uplink and downlink decoupling gains as a function of both the small cell offset factor and the distance between small cells. We have observed that the decoupling case brings higher uplink and downlink throughputs for various offset values and improves the overall system performance when being combined with a dynamic TDD technology. Furthermore, we have realized that our modeled network can be further optimized by adopting the optimal combination of both the small cell offset factor and the distance between small cells. Identifying the location of the small cell interferer and the small cell offset factor will help in improving the gain that the decoupling mode can bring to a multiple small cells TDD HetNet. This research will help provide more insight into the benefits of decoupling mode in different network deployments: single small cell and multiple small cells deployments. In addition, the provided numerical results will help in optimizing networks parameters and designing cellular network under various conditions.

An important follow-up of this work is to consider the derived analytical expressions in the design of a joint optimization algorithm and to implement these techniques in a system level simulator. The decoupling technique is a strong candidate for 5G architecture designs and it can be very useful in many systems where uplink optimization is very critical. Therefore, it is interesting to investigate the performance of the decoupling mode in 5G TDD systems with hybrid HetNet deployment, where mmWave small cells are supposed to be deployed as an overlay to traditional sub-6GHz macro cells.

References

[1] "Radio frequency (RF) system scenario (release 10)," 3GPP TS 36.211, Jun. 2012.
[2] "Further enhancements to LTE Time Division Duplex (TDD) for Downlink-Uplink (DL-UL) interference management and traffic adaptation ," 3GPP TR 36.828, Jun. 2012.
[3] J. G. Andrews, "Seven ways that HetNets are a cellular paradigm shift," *IEEE Commun. Mag.*, vol. 51, no. 3, pp. 136-144, Mar. 2013.
[4] F. Boccardi, R.W. Heath, A. Lozano, T.L. Marzetta, and P. Popovski, "Five Disruptive Technology Directions for 5G," *IEEE Communications Magazine*, Vol. 52. No. 2, 2014, pp. 74-80.
[5] K. Smiljkovikj, H. Elshaer, P. Popovski, F. Boccardi, M. Dohler, L. Gavrilovska, and R. Irmer, "Capacity analysis of decoupled down- link and uplink access in 5G heterogeneous systems," *arXiv preprint arXiv:1410.7270*, 2014.
[6] X. Liu, R. Li, K. Luo, and T. Jiang, "Downlink and uplink decoupling in heterogeneous networks for 5G and beyond," *J. Commun. Inf. Netw.*, vol. 3, no. 2, pp. 1–13, 2018.
[7] "NR; User Equipment (UE) radio transmission and reception; Part 2: Range 2 Standalone (release 16)," 3GPP TS 38.101-2, Jan. 2020.
[8] K. W. Sung, H. Haas, and S. McLaughlin, "A semi-analytical PDF of downlink SINR for femtocell networks," *EURASIP J. Wireless Commun. and Networking*, Jan. 2010.
[9] S. Plass, X. G. Doukopoulos, and R. Legouable, "Investigations on link-level inter-cell interference in OFDMA systems," *in Proc. 2006 IEEE Symposium on Communications and Vehicular Technology*, pp. 49-52.
[10] X. Yang and A. O. Fapojuwo, "Analysis of heterogeneous cellular net- work with hexagonal tessellated macrocells and randomly positioned small cells," *IEEE WCNC*, 2016.
[11] M. Taranetz and M. Rupp, "A circular interference model for wireless cellular networks," *International Wireless Communications and Mobile Computing Conference*, 2014.

[12] S. Elayoubi, B. Haddada, and B. Fourestie, "Performance evaluation of fre- quency planning schemes in OFDMA based networks," *IEEE Trans.Wireless Commun.*, vol. 7, no. 5, pp. 1623-1633, May 2008.
[13] R. Kwan and C. Leung, "On collision probabilities in frequency-domain scheduling for LTE cellular networks," *IEEE Commun. Lett.*, vol. 15, no. 9, pp. 965- 967, Sep. 2011.
[14] I. Viering, A. Klein, M. Ivrlac, M. Castaneda, and J. A. Nossek, "On uplink intercell interference in a cellular system," *in Proc. 2006 IEEE International Conference on Communications*, pp. 2095-2100.
[15] M. Ding, D. Lopez-Perez, G. Mao, and Z. Lin, "DNA-GA: A new approach of network performance analysis," *Proc. IEEE ICC 2016*,arXiv:1512.05429 [cs.IT], to be published.
[16] H. Tabassum, Z. Dawy, E. Hossain, and M. S Alouini, "A framework for uplink intercell interference modeling with channel-based scheduling," *IEEE Trans. Wireless Commun.*, vol. 12, no. 1, pp. 206-217, Jan. 2013.
[17] H. Tabassum, Z. Dawy, E. Hossain, and M. S Alouini, "Interference statistics and capacity analysis for uplink transmission in two-tier small cell networks: A geometric probability approach," *IEEE Trans. Wireless Commun.*, vol. 13, no. 7, pp. 3837-3852, Jul. 2014.
[18] Ahmad El-Hajj, Naeem Akl, Bilal Hammoud, and Zaher Dawy, "On interference modeling for the analysis of uplink/downlink interactions in TDD-OFDMA networks," *2015 International Wireless Communications and Mobile Computing Conference (IWCMC)*, pp. 497-502, 2015.
[19] B. Lahad, M. Ibrahim, S. Lahoud, K. Khawam and S. Martin,"A Statistical Model for Uplink/Downlink Intercell Interference and Cell Capacity in TDD HetNets," *in Proc. 2018 IEEE International Conference on Communications (ICC)*, 2018, pp. 1-6.
[20] F. Boccardi, J. Andrews, H. Elshaer, M. Dohler, S. Parkvall, P. Popovski, and S. Singh, "Why to decouple the uplink and downlink in cellular networks and how to do it," *arXiv preprint arXiv:1503.06746*, 2015.
[21] H. Elshaer, F. Boccardi, M. Dohler, and R. Irmer, "Downlink and uplink decoupling: a disruptive architectural design for 5G networks," *in GLOBECOM'14. IEEE*, 2014, pp. 1798-1803.
[22] "Load & backhaul aware decoupled downlink/uplink access in 5G systems," *arXiv preprint arXiv:1410.6680*, 2014.
[23] Qualcomm, "Range expansion for efficient support of heterogeneous networks," *3GPP TSG-RAN WG1 R1-083813*, 2008.
[24] K. Smiljkovikj, H. Elshaer, P. Popovski, F. Boccardi, M. Dohler, L. Gavrilovska, and R. Irmer, "Capacity analysis of decoupled down- link and uplink access in 5G heterogeneous systems," *arXiv preprint arXiv:1410.7270*, 2014.
[25] K. Smiljkovikj, P. Popovski, and L. Gavrilovska, "Analysis of the decoupled access for downlink and uplink in wireless heterogeneous networks," *Wireless Communications Letters, IEEE*, vol. 4, no. 2, pp. 173-176, 2015.
[26] W. Nie, L. Zhang, and G. Fang, "Uplink Performance Improvement by Decoupling Uplink/Downlink Access in HetNets," *IEEE Transactions on Vehicular Technology, IEEE*, vol. 66, no. 8, pp. 6862-6876, 2017.
[27] H. E. Shaer, M. N. Kulkarni, F. Boccardi, J. G. Andrews, and M. Dohler, "Downlink and Uplink Cell Association in Sub-6GHz and Millimeter Wave 5G Heterogeneous Networks," *Globecom Workshops (GC Wkshps)*, 2016 IEEE.
[28] F. Adelantado, J. Perez-Romero, and O. Sallent, "Nonuniform traffic distribution model in reverse link of multirate/multiservice wcdma-based systems," *IEEE Trans. Veh. Technol.*, vol. 56, no. 5, pp. 2902-2914,Sep. 2007.
[29] B. Lahad, M. Ibrahim, S. Lahoud, K. Khawam and S. Martin,"Analytical Evaluation of Decoupled Uplink and Downlink Access in TDD 5G HetNets," *in Proc. 2018 IEEE 29th Annual International Symposium on Personal, Indoor and Mobile Radio Communications (PIMRC)*, 2018, pp. 1-7.
[30] D. Fairthorne, "The distances between random points in two concentric circles," *Biometrika*, vol. 51, no. 1/2, pp. 275-277, Jun. 1964.
[31] "Nokia Siemens Networks, Nokia, Aspects of pico node range extension, 3GPP TSG RAN WG1 meeting 61, R1-103824," 2010.
[32] "3GPP TS 136.300, Evolved Universal Terrestrial Radio Access (EUTRA) and Evolved Universal Terrestrial Radio Access Network (EUTRAN); Overall description; Stage 2 (Release 10)," 2011.
[33] K. A. Hamdi, "A useful lemma for capacity analysis of fading interference channels," *IEEE Trans. Commun.*, vol. 58, no. 2, pp. 411-416, Feb. 2010.
[34] [3GPP TS 36.213, v11.3.0, "Evolved Universal Terrestrial Radio Access (E-UTRA); Physical layer procedures," Jun. 2013.

Bachir Lahad received the bachelor's degree in computer and communication engineering from the Faculty of Engineering at Lebanese University, Lebanon, in 2010, the Master's degree in telecommunications engineering from the Faculty of Engineering at Saint Joseph University of Beirut (USJ), Lebanon, in 2015. He is currently pursuing the Ph.D. degree with Saint Joseph University of Beirut, Lebanon and with Paris-Saclay University, France. His research interests include heterogeneous wireless networks, millimeter-wave-based communications, dynamic TDD systems, uplink/downlink decoupled access and modeling/optimization of mobile communication networks.

Marc Ibrahim is an assistant professor at Saint-Joseph University in Lebanon and the director of CIMTI (Centre Information, de Modélisation, et de Technologies de l'Information). He got his engineering degree from the Faculty of Engineering at Saint Joseph University of Beirut in Lebanon in 2002, then his Master's degree from the same faculty in 2004. In 2009, He received his PhD in communication networks from the University of Versailles in France. His research activities orbit wireless networks with a particular focus on radio resource and interference management as well as performance modeling and networks measurement.

Samer Lahoud is an Associate Professor at the Saint-Joseph University of Beirut where he lectures computer networking courses at the Faculty of engineering (ESIB). His research activities focus on routing and resource allocation algorithms for wired and wireless communication networks. He has co-authored more than 80 papers published in international journals and conference proceedings. Mr. Lahoud received the Ph.D. degree in communication networks from Telecom Bretagne, Rennes, in 2006. After his Ph.D. degree, he spent one year at Alcatel-Lucent Bell Labs Europe. From 2007 to 2016, he was with the University of Rennes 1 and with IRISA Rennes as an Associate Professor

Kinda Khawam got her engineering degree from Ecole Supérieure des Ingénieurs de Beyrouth (ESIB) in 2002, the Master's degree in computer networks from Telecom ParisTech (ENST), Paris, France, in 2003, and the Ph.D. from the same school in 2006. She was a post doctoral fellow researcher in France Telecom, Issy-Les-Moulineau, France in 2007. Actually, she is an associate professor and researcher at the University of Versailles in France. Her research interests include radio resource management, modeling and performance evaluation of mobile networks. She has co-authored more than 50 papers published in international journals and conference proceedings.

Steven Martin received his Ph.D. degree from INRIA, France, in 2004. Since 2005, Steven MARTIN is working at Paris-Sud University. Leading the research group "Networking and Optimization" at LRI (the Laboratory for Computer Science at Paris-Sud University, joint with CNRS), his research interests include quality of service, wireless networks, network coding, ad hoc networks and real-time scheduling. He is involved in many research projects and had the lead of the activity "Personal safety in digital cities of the future" in EIT ICT Labs (the European Institute of Innovation and Technology) from 2010 to 2014. He is the author of a large number of papers published in leading conference proceedings and journals. He has served as TPC member for many international conferences in networking.